Zac1 Regulates the Differentiation and Migration of Neocortical Neurons via Pac1

L. Adnani, L. Langevin, E. Gautier, R. Dixit, K. Parsons, S. Li, G. Kaushik, G. Wilkinson, R. Wilson, S. Childs, et al.

Development/Plasticity/Repair

Zac1 Regulates the Differentiation and Migration of Neocortical Neurons via *Pac1*

Lata Adnani,[1,4,5]* Lisa Marie Langevin,[1,4,5]* Elodie Gautier,[6,7] Rajiv Dixit,[1,4,5] Kari Parsons,[2,5] Saiqun Li,[1,4,5] Gaurav Kaushik,[1,4,5] Grey Wilkinson,[1,4,5] Richard Wilson,[3,4,5] Sarah Childs,[1,4] Minh Dang Nguyen,[2,5] Laurent Journot,[8] Colette Dehay,[6,7] and Carol Schuurmans[1,4,5]

Departments of [1]Biochemistry and Molecular Biology, [2]Clinical Neurosciences, and [3]Physiology and Pharmacology, [4]Alberta Children's Hospital Research Institute, [5]Hotchkiss Brain Institute, University of Calgary, Calgary, Alberta, Canada, T2N 4N1, [6]Stem Cell and Brain Research Institute, INSERM U846, 69500, Bron, France, [7]University of Lyon, University of Lyon I, 69003, Lyon, France, and [8]Institut de Génomique Fonctionnelle, UMR5203 CNRS—U661 INSERM—Université de Montpellier, 34094 Montpellier Cedex 05 France

Imprinted genes are dosage sensitive, and their dysregulated expression is linked to disorders of growth and proliferation, including fetal and postnatal growth restriction. Common sequelae of growth disorders include neurodevelopmental defects, some of which are indirectly related to placental insufficiency. However, several growth-associated imprinted genes are also expressed in the embryonic CNS, in which their aberrant expression may more directly affect neurodevelopment. To test whether growth-associated genes influence neural lineage progression, we focused on the maternally imprinted gene *Zac1*. In humans, either loss or gain of *ZAC1* expression is associated with reduced growth rates and intellectual disability. To test whether increased *Zac1* expression directly perturbs neurodevelopment, we misexpressed *Zac1* in murine neocortical progenitors. The effects were striking: *Zac1* delayed the transition of apical radial glial cells to basal intermediate neuronal progenitors and postponed their subsequent differentiation into neurons. *Zac1* misexpression also blocked neuronal migration, with *Zac1*-overexpressing neurons pausing more frequently and forming fewer neurite branches during the period when locomoting neurons undergo dynamic morphological transitions. Similar, albeit less striking, neuronal migration and morphological defects were observed on *Zac1* knockdown, indicating that *Zac1* levels must be regulated precisely. Finally, *Zac1* controlled neuronal migration by regulating *Pac1* transcription, a receptor for the neuropeptide pituitary adenylate cyclase-activating polypeptide (PACAP). *Pac1* and *Zac1* loss- and gain-of-function presented as phenocopies, and overexpression of *Pac1* rescued the *Zac1* knockdown neuronal migration phenotype. Thus, dysregulated *Zac1* expression has striking consequences on neocortical development, suggesting that misexpression of this transcription factor in the brain in certain growth disorders may contribute to neurocognitive deficits.

Key words: neocortex; neuronal migration; *Pac1*; progenitor maturation; *Zac1*

Significance Statement

Altered expression of imprinted genes is linked to cognitive dysfunction and neuropsychological disorders, such as Angelman and Prader–Willi syndromes, and autism spectrum disorder. Mouse models have also revealed the importance of imprinting for brain development, with chimeras generated with parthenogenetic (two maternal chromosomes) or androgenetic (two paternal chromosomes) cells displaying altered brain sizes and cellular defects. Despite these striking phenotypes, only a handful of imprinted genes are known or suspected to regulate brain development (e.g., *Dlk1*, *Peg3*, *Ube3a*, *necdin*, and *Grb10*). Herein we show that the maternally imprinted gene *Zac1* is a critical regulator of neocortical development. Our studies are relevant because loss of 6q24 maternal imprinting in humans results in elevated *ZAC1* expression, which has been associated with neurocognitive defects.

Introduction

Development of a functional nervous system requires that appropriate numbers of the correct types of neurons first differentiate and then migrate to their proper destinations in which they establish specific synaptic connections. Long-term cognitive and behavioral deficits can arise when neurogenesis, neuronal migration, or circuit formation are disrupted. Infants with intrauterine

Received Feb. 26, 2015; revised Aug. 21, 2015; accepted Aug. 26, 2015.

Author contributions: L.A., L.M.L., E.G., M.D.N., C.D., and C.S. designed research; L.A., L.M.L., E.G., R.D., K.P., S.L., G.K., G.W., and C.D. performed research; R.W., S.C., M.D.N., and L.J. contributed unpublished reagents/analytic tools; L.A., L.M.L., E.G., R.D., K.P., S.L., G.K., G.W., C.D., and C.S. analyzed data; L.A., L.M.L., and C.S. wrote the paper.

This project was supported March of Dimes and Canadian Institutes of Health Research Grant 89994 (C.S.). L.A., L.M.L., S.L., and G.W. were supported by a Canadian Institutes of Health Research (CIHR)/Alberta Children's Hospital Research Institute Training Grant in Genetics, Child Health, and Development. R.D. was supported by a CIHR Canada Hope Fellowship. We thank Dawn Zinyk and Nicole Gruenig for animal maintenance and Natasha Klenin for technical assistance.

growth restriction (IUGR), defined as birth weights below the 10th percentile for gestational age (Peleg et al., 1998), have an increased risk of long-term neurological disabilities (Geva et al., 2006a,b; Fattal-Valevski et al., 2009). Although IUGR-linked neurodevelopmental defects can be a secondary consequence of reduced nutrient/oxygen levels during pregnancy from placental insufficiency, several genes associated with IUGR are also expressed in the embryonic CNS, in which their dysregulated expression may more directly influence nervous system development. Included in this category are imprinted genes, which are expressed in a parent-of-origin-specific manner, and are emerging as key regulators of both intrauterine growth and brain development (Wilkinson et al., 2007; Diplas et al., 2009).

Zac1, also known as pleiomorphic adenoma gene like 1 (*Plagl1*), is a maternally imprinted gene that encodes a seven-C_2H_2 zinc finger protein (Abdollahi, 2007). Human *ZAC1* is located on chromosome 6q24-25, a locus silenced in multiple carcinomas, including head and neck, ovarian, and pituitary tumors (Abdollahi, 2007). The *ZAC1* maternal imprint is established during oogenesis by methylation of an imprinting control region (ICR), which silences transcription from a maternal P1 promoter (Arima and Wake, 2006). Loss of 6q24 maternal imprinting, resulting in biallelic expression, occurs in 70% of infants with transient neonatal diabetes mellitus (TNDM), a disorder associated with growth retardation (Temple and Shield, 2002; Azzi et al., 2014). In contrast, ICR hypermethylation reduces *ZAC1* expression in ovarian tumor cells (Kamikihara et al., 2005). Reduced *ZAC1* expression is also associated with growth restriction, developmental delay, and intellectual disability (e.g., Decipher identification numbers 248227 and 294593).

In mouse models, *Zac1* regulates embryonic growth (Varrault et al., 2006), as well as keratinocyte (Basyuk et al., 2005), heart (Czubryt et al., 2010; Yuasa et al., 2010), pancreatic islet (Anderson et al., 2009), cerebellar (Chung et al., 2011), and retinal (Ma et al., 2007a,b) development. We identified *Zac1* in a subtractive screen designed to identify new regulators of neocortical neurogenesis (Mattar et al., 2004). Here, we asked whether altered *Zac1* expression in the embryonic neocortex, the seat of higher-order cognitive functioning, could give rise to morphological defects that may result in neurocognitive deficits (Geva et al., 2006a,b; Fattal-Valevski et al., 2009). Misexpression of *Zac1* in neocortical progenitors inhibited progenitor maturation, while delaying neuronal differentiation and migration. The effects of *Zac1* on neuronal migration were in part mediated by *Pac1* (*pituitary adenylate cyclase-activating polypeptide type I receptor*), a *Zac1* transcriptional target (Ciani et al., 1999; Rodríguez-Henche et al., 2002) that controls neocortical progenitor proliferation (Suh et al., 2001; Yan et al., 2013). We have thus identified a novel *Zac1–Pac1* regulatory pathway that controls progenitor maturation, neuronal differentiation, and migration in the developing neocortex.

Materials and Methods

Animals. Embryos were staged using the morning of the vaginal plug as embryonic day 0.5 (E0.5). CD1 mice (Charles River Laboratories) were used for *in utero* electroporation experiments. *Zac1* null mutant embryos were obtained by crossing $Zac1^{+/-}$ males with C57BL/6 wild-type females. The resulting $Zac1^{+m/-}$ embryos, which obtained their wild-type allele from the dam, were the equivalent of *Zac1* null mutants because of imprinting of the maternal *Zac1* allele. Genotyping *Zac1* mutant and wild-type alleles was performed as described previously (Ma et al., 2007b).

Constructs used for in utero *electroporation.* For gain-of-function experiments, *Zac1* and *Pac1* were cloned into pCIG2 (Hand et al., 2005), a bicistronic expression vector containing a β-actin promoter/CMV enhancer and an internal ribosome entry site (IRES)–EGFP cassette (Hand et al., 2005). For knockdown experiments, shRNAs were obtained from ORIGENE: HuSH shRNA TG502444 *Mus musculus Plagl1* (*Zac1*) in pGFP–V-RS; HuSH shRNA TG500044 *M. musculus Adcyap1r1* in pGFP–V-RS. To identify which of the four shRNAs was most effective, NIH-3T3 cells were transfected with pCIG2–*Zac1* or pCIG2–*Pac1* either alone or together with individual shRNAs, and Western blots were performed 24 h later (as in the study by Li et al., 2012). The scrambled shRNA was from ORIGENE (TR30013). EGFP–CentII (Tanaka et al., 2004) and pEF/Myc/ER/GFP vectors (Invitrogen) were modified to incorporate RFP and mCherry reporters, as described previously (Shim et al., 2008).

In utero *electroporation. In utero* electroporation was performed as described previously (Dixit et al., 2011). Briefly, endotoxin-free DNA was prepared according to the instructions of the manufacturer (Qiagen) and injected at 1.5 μg/μl into the telencephalic vesicles of embryos in time-staged pregnant females anesthetized under inhalable isoflurane (5 L/min) using a Femtojet microinjector apparatus (VWR CanLab) and three-axis coarse manipulator (Carl Zeiss). This was followed by seven 50 V pulses at 750 ms intervals applied by tweezer-style electrodes (5 mm for E12.5 and 7 mm for E14.5; Protech International) using a BTX square wave electroporator (VWR CanLab). The uterus was replaced in the body cavity, the peritoneum was sutured, the skin stapled, and normal embryonic development proceeded until the time of harvesting.

RNA extraction, cDNA synthesis, and quantitative real-time PCR. RNA was extracted from E18.5 wild-type and *Zac1* mutant cortices and from microdissected E13.5–E14.5 cortical tissue electroporated with pCIG2 or pCIG2–*Zac1* using an RNeasy Mini kit (Qiagen) according to the instructions of the manufacturer. First-strand cDNA was synthesized using the Quantitect Reverse Transcription kit (Qiagen) according to the instructions of the manufacturer. Real-time qRT-PCR was performed using an Opticon 2 DNA engine (Bio-Rad Laboratories) using a Quantifast SYBR Green kit (Qiagen). For every primer pair, three different cDNA dilutions were tested with the following cycle conditions: one cycle of 95°C for 4 min, 40 cycles of 95°C for 1 min, 55–67°C for 1 min, 72°C for 1 min 30 s, and one cycle of 72°C for 10 min. The annealing temperature was optimized for each primer pair using a temperature gradient, selecting conditions that yielded >95% amplification efficiencies. Normalization was achieved using hypoxanthine phosphoribosyl-transferase 1 (*Hprt*) and *Beta-2 microglobulin* (*B2m*) as reference genes: *Pac1* forward, TACTCCAGATGTGGTTCCAGGC; *Pac1* reverse, AGTGAGGTCCG TGGGGTTTATC (66°C annealing); *B2M* forward, CCTGGTCTTT CTGGTGCTTGTC; *B2M* reverse, CAGTATGTTCGGCTTCCCATTC (63°C annealing); *HPRT* forward, AGCTACTGTAATGATCAGTCA ACG; *HPRT* reverse, AGAGGTCCTTTTCACCAGCA (58.3°C annealing); *Zac1* forward, AATGTGGCAAGTCCTTCGTCAC; and *Zac1* reverse, TGGTTCTTCAGGTGGTCCTTCC (67°C annealing).

Tissue processing and immunolabeling. Dissected brains were fixed overnight at 4°C in 4% paraformaldehyde (PFA)/1× PBS. Brains were rinsed three times for 10 min in 1× PBS and transferred to 20% sucrose/1× PBS overnight at 4°C. Cryopreserved brains were then embedded in O.C.T. (Tissue-Tek; Sakura Finetek) and stored at −80°C before cutting 10 μm cryosections. For immunolabeling, sections were blocked 1 h in 10% normal goat serum in 1× TBST (Tris-buffered saline: 25 mM Tris, 0.14 M NaCl, and 0.1% Triton X-100) at room temperature. Primary antibodies were diluted in blocking solution and incubated on slides overnight at 4°C. Slides were washed three times for 10 min in TBST before incubating in secondary antibody diluted in TBST for 1 h at room temperature. Nuclei were counterstained in 4′,6-diamidino-2-phenylindole (DAPI; Santa Cruz Biotechnology) diluted 1:10,000 in 1× PBS for 5 min and then destained with three PBS washes for 5 min before mounting in AquaPolymount (Polysciences). Primary antibodies included the following: mouse anti-BrdU (1:200; Roche Diagnostics),

*L.A. and L.M.L. contributed equally to this work.

The authors declare no competing financial interests.

Correspondence should be addressed to Carol Schuurmans, University of Calgary, 3330 Hospital Drive NW, Calgary, Alberta, Canada, T2N 4N1. E-mail: cschuurm@ucalgary.ca.

DOI:10.1523/JNEUROSCI.0777-15.2015

 0270-6474/15/3513431-18$15.00/0

rabbit anti-GFP (1:500; Millipore Bioscience Research Reagents), rabbit anti-Pax6 (1:500; Covance), rabbit anti-Cux1 (anti-CDP; 1:500; Santa Cruz Biotechnology), mouse anti-Tuj1 (Neuronal class III β-tubulin; 1:500; Covance), rabbit anti-Tbr1 (1:3000; Millipore Bioscience Research Reagents), rabbit anti-Tbr2 (1:500; Abcam), rabbit anti-phospho-histone H3 (pHH3; 1:1000; Millipore Biotechnology), mouse anti-neuronal-specific nuclear protein (NeuN; 1:500; Millipore Bioscience Research Reagents), goat anti-Beta3 (1:300; Santa Cruz Biotechnology), rat anti-Ctip2 (1:100; Abcam), rabbit anti-Ki67 (1:200; Abcam), and rabbit anti-Zac1 (1:1000; Spengler et al., 1997). Secondary antibodies were conjugated to Alexa Fluor 488 (1:500; Invitrogen) or Cy3 (1:500; Jackson ImmunoResearch).

BrdU and 5-ethynyl-2′-deoxyuridine labeling. For birthdating and proliferation studies, 100 μg/g body weight BrdU (Sigma) was injected intraperitoneally at E14.5. For BrdU immunolabeling, sections were treated with 2N HCl for 25 min at 37°C before processing (Britz et al., 2006). Cell proliferation was assayed via 5-ethynyl-2′-deoxyuridine (EdU) staining, using the Click-iT EdU Alexa Fluor 594 kit (Invitrogen). Two hundred microliters 1 μg/μl EdU dissolved in PBS was injected subcutaneously into pregnant dams 30 min before they were killed. For gain-of-function studies, sections were first stained with αGFP and post-fixed for 1 h in 4% PFA/1× PBS at 4°C. Slides were the rinsed three times for 10 min in 5% bovine serum albumin/1× PBS and then stained for EdU as per the instructions of the manufacturer. Slides were rinsed three times for 5 min in 1× PBS, counterstained with DAPI, and mounted using Aqua Polymount.

Biphoton time-lapse video microscopy. E15.5 cortices were dissected and electroporated with pCIG2 (control) or pCIG2–*Zac1* expression constructs. Briefly, 1.5 μl of plasmid at 1–2 μg/μl was mixed with Fast Green (0.01 mg/ml; Sigma) and injected into the lateral ventricles of whole heads using a Hamilton syringe. Gold electrodes (Genetrode BTX model 514; Harvard Apparatus) were used to deliver five pulse of 30 V, 50 ms on/1000 ms off. The anode was oriented dorsally and the cathode ventrally. Cortices were then sliced and maintained in culture for 4 d (37°C, 7.5% CO_2) as 150 μm organotypic slices. Biphoton time-lapse video microscopy was performed on 24 recorded positions in both hemispheres of 12 brain slices (two from each brain, $n = 3$ for each construct) over 3 d beginning 30 h after electroporation. One image was taken per hour on 100 μm with 20 *z* slices. A total of 195 control neurons (pCIG2) and 133 *Zac1*-transfected neurons were traced. Migration parameters extracted for each neuron included time of departure and arrival (number of hours after electroporation), migration duration (*T*, in hours), distance (*D*, in micrometers), velocity (micrometers per hours, *D*/*T*), and number and duration of pauses during saltatory locomotion. A pause was defined as nonsignificant movement (<3.5 μm) during at least 2 consecutive hours. Migration parameters were calculated for each neuron on a fragmented track. The neocortex thickness was subdivided into 20 bins parallel to the ventricular border, and the values were calculated for movements made in each bin. As neurons can begin and finish their track in different bins, only bins with at least half of the population making a part of their tracks in a bin were taken into account.

RNA in situ *hybridization.* RNA *in situ* hybridization was performed as described previously (Touahri et al., 2015). The *Zac1* digoxygenin-labeled riboprobe was generated as described previously (Alam et al., 2005).

Imaging, tracing, quantitation, and statistics. Images were captured with a QImaging RETIGA 2000R or QImaging RETIGA EX digital camera and a Leica DMRXA2 optical microscope using OpenLab5 software (Improvision). Confocal images were acquired using a Nikon C1si Spectral confocal microscope. Using these images, neurons were traced with the paint tool in Photoshop CS6 (64 bit; Adobe Systems). Cell counts were performed on a minimum of three embryos per genotype or treatment group and a minimum of three cortical sections from each embryo. Statistical significance was calculated using a Student's *t* test when comparing two values, and three or more values were compared using a two-way ANOVA with a Bonferroni's correction unless indicated. Graphs and statistics were generated using GraphPad Prism Software (GraphPad Software). Error bars represent SEM. *p* values were denoted as follows: $*p < 0.05$, $**p < 0.01$, and $***p < 0.005$.

Results

Overexpression of *Zac1* in neocortical progenitors perturbs late-born neuronal migration

Previous analyses revealed that *Zac1* is expressed in a regionalized manner in the developing nervous system, including in the telencephalon, the anlage of the neocortex (Alam et al., 2005). To better understand how *Zac1* might function during neocortical development, we assessed its expression in this region of the embryonic neural tube in more detail. At E12.5, *Zac1* transcripts were detected at high levels in dorsal telencephalic (neocortical) progenitor cells in the ventricular zone (VZ) and at lower levels in the ventral telencephalic VZ (Fig. 1*A*,*A*′). At E15.5, *Zac1* continued to be expressed in neocortical VZ progenitors, as well as in deep layers of the developing cortical plate (CP; Fig. 1*B*,*B*′). A similar spatiotemporal distribution was observed using Zac1-specific antisera; at E12.5 (Fig. 1*C*,*C*′) and E14.5 (Fig. 1*D*,*D*′), Zac1 protein was detected in most neocortical VZ progenitors but not in postmitotic $Tuj1^+$ neurons. By E16.5 (Fig. 1*E*,*E*′,*E*″) and at E18.5 (Fig. 1*F*,*F*′,*F*″), Zac1 protein continued to be expressed widely in the neocortical VZ and could now be detected in a small number of subventricular zone (SVZ) cells and deep layer neurons. Thus, Zac1 is expressed primarily in neocortical VZ progenitors and in a smaller number of SVZ progenitors and deep layer postmitotic neurons.

To mimic the upregulation of *Zac1* expression associated with loss of the maternal imprint in TNDM, a bicistronic pCIG2–*Zac1* expression vector containing an IRES–EGFP cassette or an empty vector pCIG2 control were introduced into E12.5 and E14.5 neocortical progenitors via *in utero* electroporation. The positions of GFP-expressing (GFP^+) electroporated cells were then assessed at E18.5. Control and *Zac1* E12.5–E18.5 electroporations looked similar, with most GFP^+ electroporated cells concentrated in deep neocortical layers ($n = 3$; $p > 0.05$ comparing all layers; Fig. 1*G–I*), in accordance with the E12.5 birthdate of layer VI neurons (Caviness, 1982; Caviness et al., 1995). In contrast, a striking migratory block was observed in E14.5–E18.5 *Zac1* electroporations, with *Zac1*-overexpressing cells aggregating in the intermediate zones (IZs; $n = 6$; $p < 0.01$) instead of migrating into upper ($n = 6$; $p < 0.005$) layers of the CP (Fig. 1*J–L*). Thus, overexpression of *Zac1* strongly perturbs cellular migration at later stages of neocortical development, either because overexpressing cells fail to differentiate and/or because *Zac1* impairs neuronal migration, which we addressed further below.

Zac1 misexpression delays progenitor cell maturation and neuronal differentiation

To further dissect the effects of *Zac1* overexpression on neocortical progenitors, we focused on E14.5 electroporations, when *Zac1*-induced migratory defects were most profound. At E14.5, $Pax6^+$ radial glial cell (RGC) progenitors in the VZ give rise to $Tbr2^+$ intermediate neuronal progenitors (INPs) in the SVZ, which divide once or twice before differentiating into $Tbr1^+$ neurons (Noctor et al., 2004; Fig. 2*A*). To test whether *Zac1* overexpression perturbed the RGC-to-INP transition, we performed shorter E14.5–E15.5 electroporations. By 24 h after electroporation, the vast majority of pCIG2-transfected GFP^+ progenitors migrated to the upper VZ/SVZ, in transition to becoming an INP (Fig. 2*B*,*D*). In contrast, more *Zac1*-transfected cells remained in the lower VZ ($n = 3$; $p < 0.005$), and many fewer cells reached the SVZ ($n = 3$; $p < 0.005$; Fig. 2*C*,*D*), consistent with a possible block in the RGC-to-INP transition.

A distinguishing feature of RGC progenitors is their cell cycle-dependent interkinetic nuclear movements, with nuclei in G_2/M-

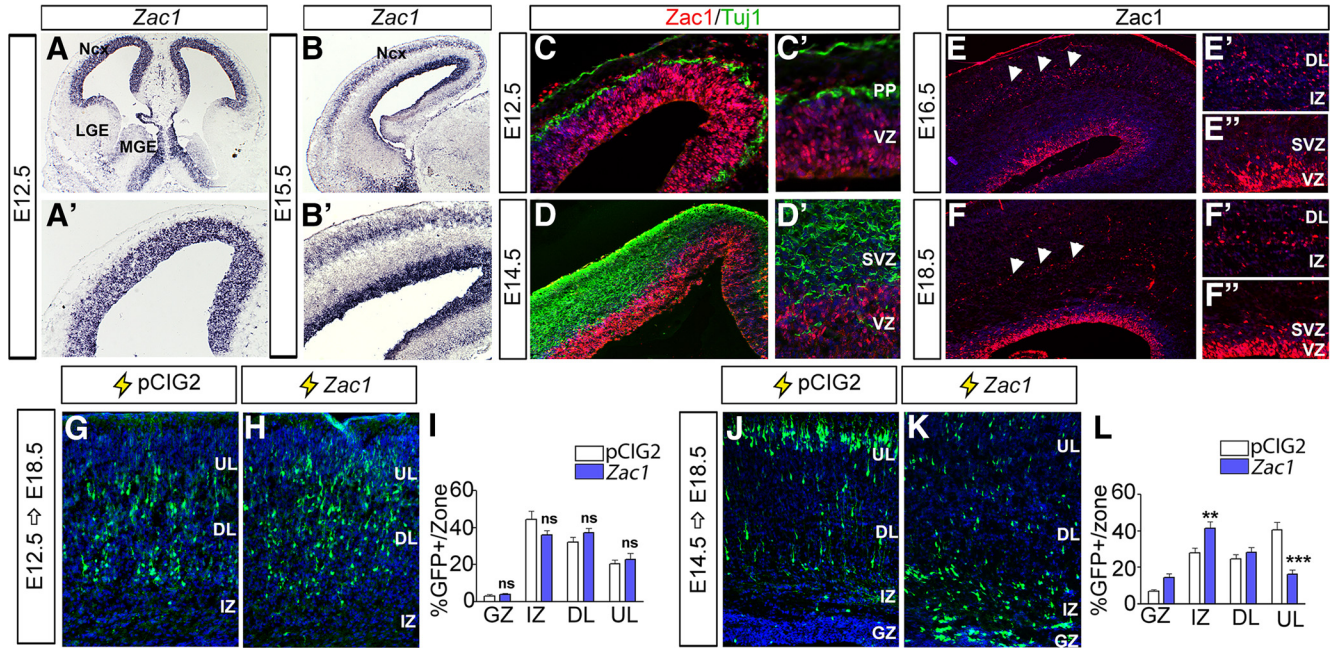

Figure 1. *Zac1* overexpression perturbs cell migration during later stages of corticogenesis. ***A***, ***B***, *Zac1* transcript distribution in E12.5 (***A***, ***A′***) and E15.5 (***B***, ***B′***) telencephalon. ***A′*** and ***B′*** are high-magnification images of ***A*** and ***B***, respectively. ***C–F***, Distribution of Zac1 (red, ***C–F″***) and Tuj1 (green, ***C***, ***D***) protein in the E12.5 (***C***, ***C′***), E14.5 (***D***, ***D′***), E16.5 (***E–E″***), and E18.5 (***F–F″***) neocortex. ***C′–F′*** are higher-magnification images of ***C–F***, respectively. Arrowheads in ***E*** and ***F*** mark CP expression. Comparison of E12.5–E18.5 (***G–I***) and E14.5–E18.5 (***J–L***) electroporations of pCIG2 control (***G***, ***J***) and pCIG2-*Zac1* (***H***, ***K***) analyzed for the distribution of GFP$^+$ cells/zone (***I***, ***L***).

phase of the cell cycle dividing at the apical surface, whereas INP mitoses occur in basal positions. To determine whether *Zac1* influenced the apical-to-basal mitotic transition, we examined the expression of pHH3, a G_2/M-phase marker (Fig. 2*E–G*). In E14.5–E15.5 transfections, of the *Zac1*-transfected (GFP$^+$) cells that coexpressed pHH3, most divided in apical regions of the VZ ($n = 3$; $p < 0.005$), whereas fewer divided basally compared with control pCIG2 transfections ($n = 3$; $p < 0.005$; Fig. 2*G*). These data are consistent with the idea that *Zac1* maintains an RGC identity while blocking the transition to an INP fate. To provide additional support for this conclusion, we examined the expression of Pax6 and Tbr2, which are expressed specifically in, and are essential determinants of, RGC and INP progenitor cell fates, respectively (Englund et al., 2005; Sessa et al., 2008). At 24 h after E14.5 electroporation, significantly more *Zac1*-misexpressing cells versus control-transfected cells expressed Pax6 ($n = 3$; $p < 0.01$; Fig. 2*H–J*). Concomitantly, fewer *Zac1*-transfected cells expressed Tbr2 ($n = 3$; $p < 0.005$; Fig. 2*K–M*). Thus, *Zac1* misexpression blocks the maturation of cortical progenitors from an apical Pax6$^+$ RGC identity to a basal Tbr2$^+$ INP fate.

The delay in progenitor cell maturation associated with *Zac1* overexpression suggested that this transcription factor may also block neuronal differentiation. To assess the effects of *Zac1* on neuronal differentiation, we examined the expression of Tbr1 (Fig. 2*N–P*), a T-box transcription factor that is expressed at high and low levels, respectively, in deep and upper layer cortical neurons (Englund et al., 2005). In E14.5–E15.5 electroporations, the number of *Zac1*-transfected cells that expressed Tbr1 was reduced compared with control transfections ($n = 3$; $p < 0.05$; Fig. 2*P*). These data suggest that *Zac1* does indeed block neuronal differentiation in the neocortex. However, these results were somewhat unexpected, because *Zac1* promotes cell-cycle exit when misexpressed in cell lines (Spengler et al., 1997; Schmidt-Edelkraut et al., 2014) or in the retina (Ma et al., 2007b), and exit from the cell cycle is a hallmark feature of neuronal differentiation. To test whether *Zac1* influenced the proliferative capacity of E14.5 cortical progenitor cells, we performed a 30 min pulse label with the thymidine analog EdU (Fig. 2*Q–S*). In E14.5–E15.5 electroporations of *Zac1*, fewer GFP$^+$EdU$^+$/GFP$^+$ proliferating S-phase progenitors were detected compared with pCIG2 control transfections ($n = 3$; $p < 0.05$). To confirm that *Zac1*-misexpressing cells exited the cell cycle at a higher frequency, we administered BrdU immediately after electroporation of pCIG2 or *Zac1* at E14.5. At E15.5, 24 h after electroporation, embryos were harvested and quantified based on the number of electroporated GFP$^+$ cells that incorporated BrdU while also expressing Ki67 (Fig. 2*T–V*). This value gave us a measure of the number of GFP$^+$ cells that were proliferating at the time of electroporation and also remained in the cell cycle 24 h later. The number of cells that remained in the cell cycle 24 h after electroporation was reduced when *Zac1* was overexpressed ($n = 3$) compared with pCIG2 ($n = 3$; $p < 0.05$; Fig. 2*V*). Thus, *Zac1* promotes cell-cycle exit in cortical progenitors, although it does not initiate the expression of neuronal differentiation markers such as Tbr1.

Zac1 overexpression reduces the expression of neuronal differentiation markers

To test whether *Zac1* overexpression blocked as opposed to delayed the expression of neuronal differentiation markers, we extended the time after which E14.5 electroporated brains were analyzed to E18.5 (Fig. 3*A–P*). Four days after electroporation, NeuN (neuronal nuclear antigen), which is a late neuronal marker, was expressed in comparatively fewer *Zac1*- versus control-transfected cells ($n = 3$; $p < 0.005$; Fig. 3*A–C*), particularly in the germinal zone (GZ; $n = 3$; $p < 0.01$; Fig. 3*D*). Notably, the overall number of GFP$^+$NeuN$^+$ cells was low even in control transfections because NeuN was not expressed at high levels in

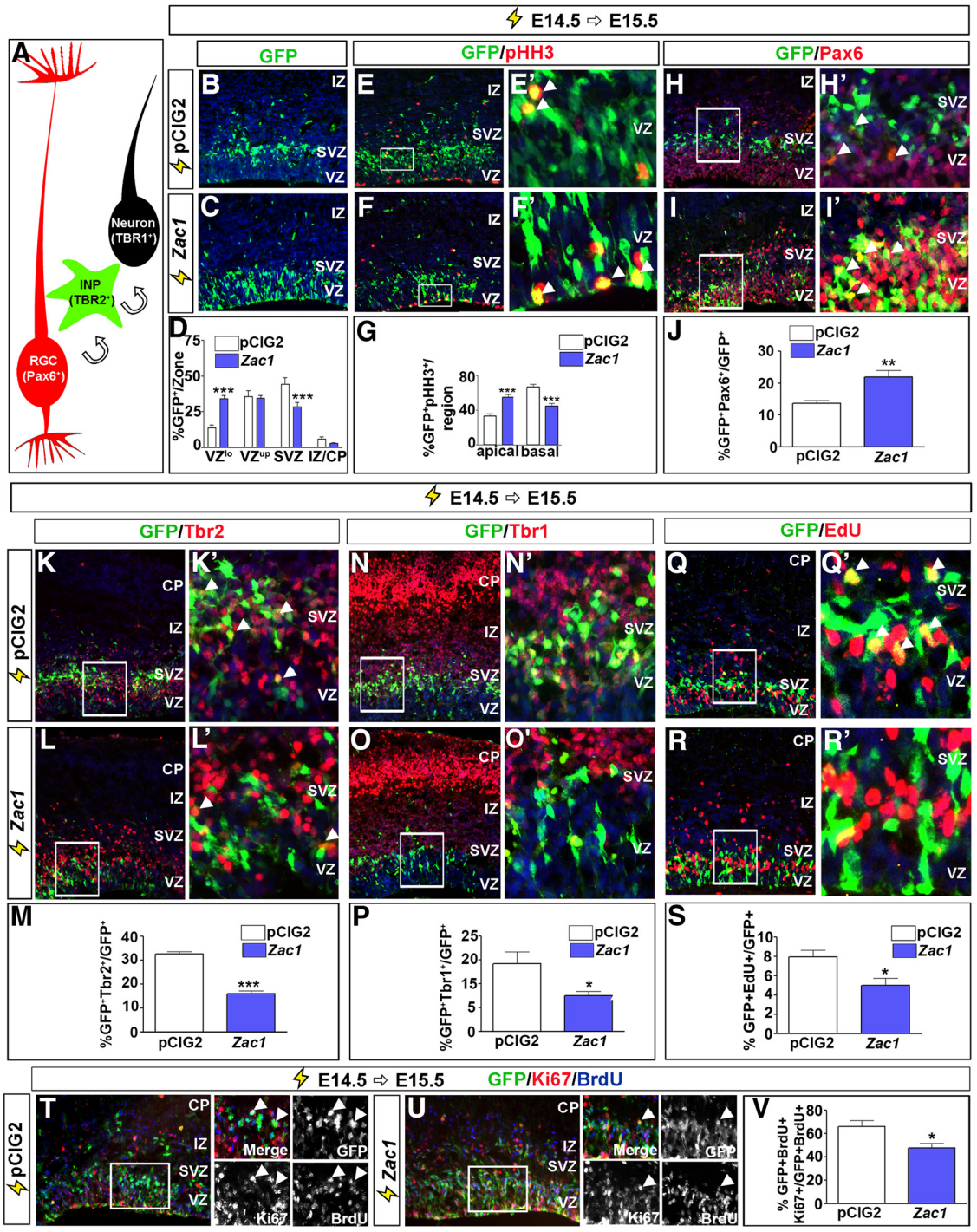

Figure 2. *Zac1* overexpression delays progenitor cell maturation and neuronal differentiation. ***A***, Schematic illustration of cells transitioning from Pax6$^+$ RGCs to Tbr2$^+$ INPs to Tbr1$^+$ differentiated neurons. ***B–S***, E14.5–E15.5 electroporations of pCIG2 control (***B***, ***E***, ***H***, ***K***, ***N***, ***Q***) and pCIG2–*Zac1* (***C***, ***F***, ***I***, ***L***, ***O***, ***R***) costained for GFP and pHH3 (***E***, ***E′***, ***F***, ***F′***), GFP and Pax6 (***H***, ***H′***, ***I***, ***I′***), GFP and Tbr2 (***K***, ***K′***, ***L***, ***L′***), GFP and Tbr1 (***N***, ***N′***, ***O***, ***O′***), and GFP and EdU (***Q***, ***Q′***, ***R***, ***R′***). ***E′***, ***F′***, ***H′***, ***I′***, ***K′***, ***L′***, ***N′***, ***O′***, ***R′***, and ***Q′*** are high-magnification images of boxed regions in ***E***, ***F***, ***H***, ***I***, ***K***, ***L***, ***N***, ***O***, ***R***, and ***Q***, respectively. Arrowheads in ***E′***, ***F′***, ***H′***, ***I′***, ***K′***, ***L′***, and ***Q′*** mark double-positive cells. Quantitation of GFP$^+$ cells/zone (***D***), percentage pHH3$^+$GFP$^+$ mitotic cells in apical and basal regions of the cortex (***G***), percentage Pax6$^+$GFP$^+$/GFP$^+$ cells (***J***), percentage Tbr2$^+$GFP$^+$/GFP$^+$ cells (***M***), percentage Tbr1$^+$GFP$^+$/GFP$^+$ cells (***P***), and percentage EdU$^+$ GFP$^+$/GFP$^+$ cells (***S***) after the electroporation of pCIG2 (white bars, $n = 3$) and pCIG2–*Zac1* (blue bars, $n = 3$). ***T–V***, E14.5–E15.5 electroporations of pCIG2 control (***T***) and pCIG2-*Zac1* (***U***) costained for GFP (green), Ki67 (blue), and BrdU (red) after a 24 h BrdU pulse. Quantitation of percentage Ki67$^+$BrdU$^+$GFP$^+$/GFP$^+$BrdU$^+$ cells (***V***). Arrowheads in ***T*** and ***U*** point to BrdU$^+$ proliferating cells that have been electroporated (GFP$^+$) and have remained in the cell cycle (Ki67$^+$). DAPI labeling is in blue for ***B–R′***.

upper layers of the neocortex. Thus, we also examined the effects of *Zac1* misexpression on the differentiation of deep layer (Ctip2) and upper layer (Cux1 and Beta3) neurons using cell type-specific markers. Ctip2 is expressed in layer V neurons, most of which differentiate before E14.5. Accordingly, <6.0 ± 0.8% of GFP$^+$ neurons in pCIG2 control electroporations expressed Ctip2 (Fig. 3*E*,*G*), and even fewer GFP$^+$Ctip2$^+$ neurons were observed during *Zac1* overexpression ($n = 3$; $p < 0.01$), particularly in deep layers of the CP ($n = 3$; $p < 0.005$; Fig. 3*H*). Consistent with the idea that E14.5 progenitors preferentially

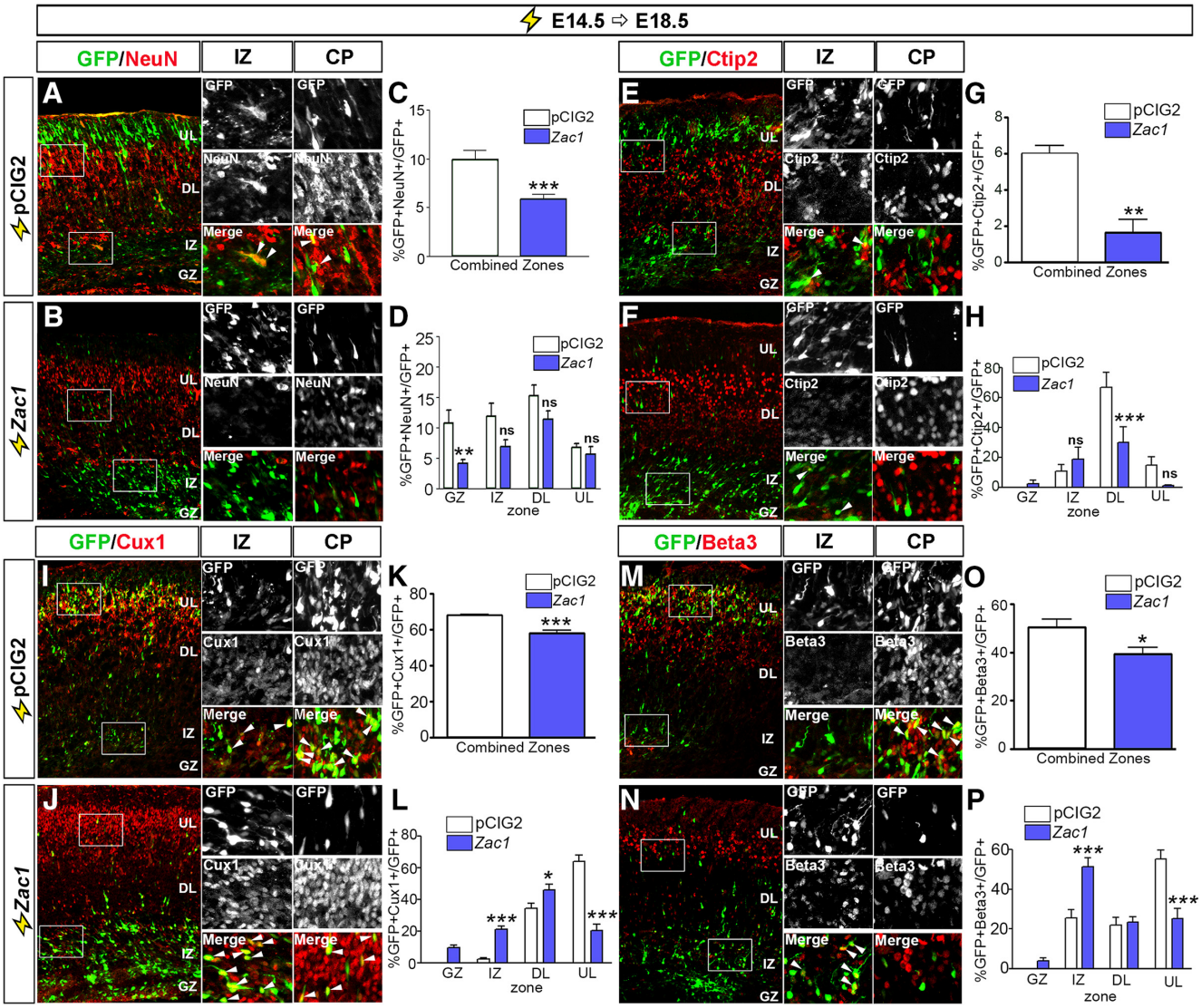

Figure 3. *Zac1* overexpression blocks neuronal differentiation. ***A–P***, E14.5–E18.5 electroporations of pCIG2 control (***A***, ***E***, ***I***, ***M***) and pCIG2–*Zac1* (***B***, ***F***, ***J***, ***N***) analyzed for the expression of GFP and NeuN (***A***, ***B***), GFP and Ctip2 (***E***, ***F***), GFP and Cux1 (***I***, ***J***), and GFP and Beta3 (***M***, ***N***). Insets to the right are high-magnification images of boxed regions in the IZ and CP in ***A***, ***B***, ***E***, ***F***, ***I***, ***J***, ***M***, and ***N***, and arrowheads mark double-positive cells. Quantitation of percentage NeuN $^+$GFP $^+$/GFP $^+$ cells in total (***C***) and per zone (***D***), Ctip2 $^+$ GFP $^+$/GFP $^+$ cells in total (***G***) and per zone (***H***), Cux1 $^+$ GFP $^+$/GFP $^+$ cells in total (***K***) and per zone (***L***), and Beta3 $^+$ GFP $^+$/GFP $^+$ cells in total (***O***) and per zone (***P***) after the electroporation of pCIG2 (white bars, $n = 3$) and pCIG2–*Zac1* (blue bars, $n = 3$).

differentiate into upper layer neurons, many more control transfected cells expressed Cux1 (Fig. 3*I*,*K*) and Beta3 (Fig. 3*M*,*O*), markers for upper layers II–IV and II–V, respectively. *Zac1* misexpression reduced the number of progenitors that differentiated into both Cux1 $^+$ ($n = 3$; $p < 0.005$; Fig. 3*I–K*) and Beta3 $^+$ ($n = 3$; $p < 0.05$; Fig. 3*M–O*) neurons, particularly in upper neocortical layers [Cux1, $n = 3$, $p < 0.005$ (Fig. 3*L*); Beta3, $n = 3$, $p < 0.005$ (Fig. 3*P*)]. More Cux1 $^+$ and Beta3 $^+$ neurons were also observed in the IZ during *Zac1* misexpression [$n = 3$ for both; $p < 0.005$ for Cux1 (Fig. 3*L*) and $p < 0.005$ for Beta3 (Fig. 3*P*)], suggesting that some neurons differentiate when *Zac1* is overexpressed, but these neurons fail to migrate to their correct position in the CP.

Together, these data suggest that there is a block in neuronal differentiation in a subset of *Zac1*-overexpressing progenitors, whereas many of the neurons that differentiate fail to migrate to their correct location in the CP.

Zac1-overexpressing cells exhibit decreased migratory velocities and increased pause time

Defects in the migration of *Zac1*-overexpressing neurons were evident 96 h after transfection of E14.5 cortical progenitors (Fig. 1*J–L*). To better assess the effects of *Zac1* misexpression on the migratory behavior of differentiating neurons, we used time-lapse biphoton laser scanning microscopy to image transfected cells in real time after *ex utero* electroporation of E15.5 cortical slices. Recordings were initiated 30 h after electroporation and were continued over 3 d with one image taken per hour. In total, 133 control ($n = 3$) and 195 ($n = 3$) *Zac1*-misexpressing cells were traced through 71 positions along the radial cortical axis, with video microscopy ending at 101 h after electroporation (Fig. 4*A*,*B*). Newly born neurons generated at E15.5 were expected to exit the GZ within 48 h (Langevin et al., 2007), but a large proportion (63.7% by 72 h) of *Zac1*-electroporated cells did not exit the GZ until 72 h after transfection compared with controls

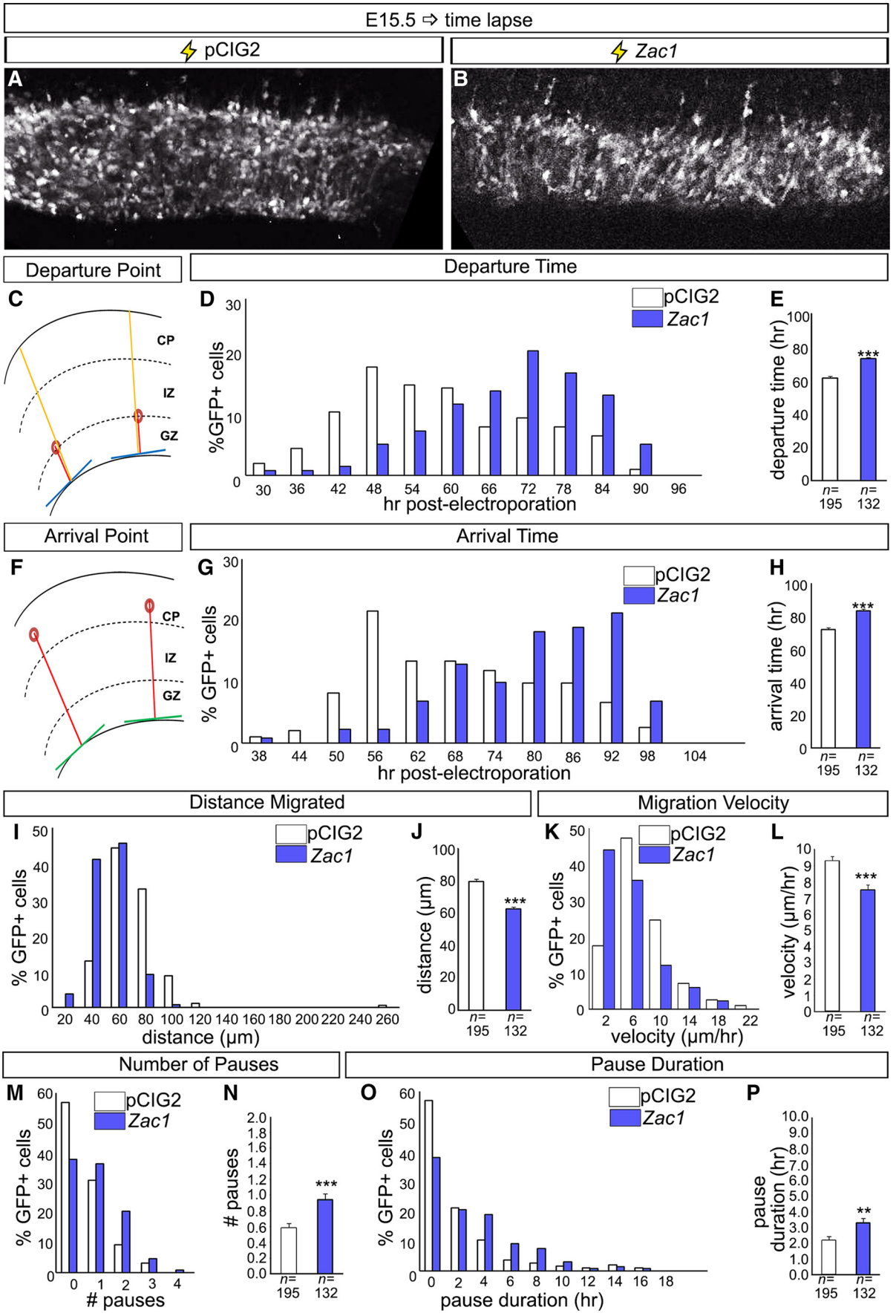
E15.5 ⇨ time lapse
pCIG2
Zac1
A
B
Departure Point
Departure Time
C
D
E
CP
IZ
GZ
pCIG2
Zac1
%GFP+ cells
hr post-electroporation
departure time (hr)
***
n= 195
n= 132
Arrival Point
Arrival Time
F
G
H
arrival time (hr)
Distance Migrated
Migration Velocity
I
J
K
L
% GFP+ cells
distance (μm)
velocity (μm/hr)
Number of Pauses
Pause Duration
M
N
O
P
pauses
pause duration (hr)
**

(66.3% by 60 h; Fig. 4*C*,*D*). Thus, on average, the peak departure time, defined as the time when neurons left the GZ and entered the IZ (Fig. 4*C*), occurred significantly later in *Zac1*-misexpressing cells compared with controls ($p < 0.005$; Fig. 4*D*,*E*). As migration proceeded, a large subset of control cells (32.8%) managed to arrive at the CP within 56 h after transfection, whereas most *Zac1*-overexpressing cells (53.1%) took in excess of 80 h to complete this phase of migration (Fig. 4*F*,*G*). Accordingly, the peak arrival time of *Zac1*-misexpressing cells in the CP was delayed ($p < 0.005$; Fig. 4*H*), and the overall distance migrated was reduced from 79.6 ± 1.7 μm for control cells to 62.8 ± 1.2 μm for *Zac1*-transfected cells ($p < 0.005$; Fig. 4*I*,*J*). *Zac1* overexpression also affected migration velocity, with *Zac1*-transfected cells (43.9%) averaging a velocity of ~7.5 ± 0.3 μm/h compared with control cells, which migrated on average at 9.3 ± 0.3 μm/h ($p < 0.005$; Fig. 4*K*,*L*).

Locomotion is a saltatory, discontinuous process whereby neurons undergo periods of active movement interspersed by pauses (Nadarajah et al., 2001, 2003). *Zac1*-misexpressing cells paused more often (25.0% of cells paused two or more times) during migration when compared with the migratory progress of control cells (12.3% paused two or more times; $p < 0.005$; Fig. 4*M*,*N*), and the length of their pauses was longer compared with control transfected cells ($p < 0.01$; Fig. 4*O*,*P*). The motility index, defined as the migration capacity of each cell without considering pauses, was also reduced in *Zac1*-misexpressing cells (*Zac1*, 11.1 ± 0.3 μm/h vs pCIG2, 11.9 ± 0.2 μm/h).

Together, these data indicate that *Zac1* overexpression in neocortical progenitors reduces migratory velocity and increases pause time and frequency.

Zac1-overexpressing neurons exhibit aberrant morphologies

Cortical neurons undergo a series of morphological transitions as they differentiate and migrate, the perturbation of which can block radial migration. To examine whether *Zac1* misexpression influenced the morphology of migrating neurons, we used spectral confocal microscopy to image transfected neurons after E14.5–E18.5 electroporations of pCIG2 and *Zac1* (Fig. 5*A*–*I*). Cortical neurons born at E14.5 use glial-guided locomotion to migrate, with their leading process contacting RGCs, which serve as glial guides. As differentiating neurons exit the GZ, they initially stall in the upper SVZ and IZ, in which they acquire a transient multipolar morphology that is associated with the dynamic extension and retraction of neurites (Tabata and Nakajima, 2003; Noctor et al., 2004). This is followed by the acquisition of a motile, bipolar morphology, with neurons extending a leading process toward the pial surface and a smaller lagging process oriented toward the ventricle (Nadarajah et al., 2001; Noctor et al., 2004). Because the waiting or pause period was increased after *Zac1* misexpression, we questioned whether the multipolar-to-bipolar transition was disrupted. We first traced 82 pCIG2-transfected and 137 *Zac1*-transfected Tuj1$^+$ neurons in the IZ ($n = 3$). In both pCIG2 and *Zac1* electroporations, many Tuj1$^+$ neurons in the IZ had a multipolar phenotype (34.4 ± 6.7% for pCIG2 and 36.4 ± 5.5% for *Zac1*), but the vast majority of neurons had transited to typical unipolar or bipolar neuronal morphologies (65.6 ± 6.7% for pCIG2 and 53.6 ± 4.6% for *Zac1*), with processes extending toward the apical (ventricular) and basal (pial) surfaces (Fig. 5*A*,*A*′,*E*,*F*). However, although most pCIG2-transfected neurons extended neurites (99.8 ± 0.2%), 10.4 ± 2.6% of *Zac1*-overexpressing neurons in the IZ lacked any detectable processes, instead acquiring an amorphous cell shape ($p < 0.01$; Fig. 5*B*,*B*′,*G*). Thus, *Zac1* overexpression perturbs the ability of cortical neurons to extend processes in the IZ (Fig. 5*G*).

Once locomoting neurons reach their destination in the CP, their leading process extends multiple branches that attach to the pial surface, providing traction for the rapid pulling of neurons into their final laminar position in a process known as somal translocation (Nadarajah et al., 2001). To determine whether *Zac1* misexpression perturbed these late morphological changes, we examined the morphology of neurons in upper layer II/III of the CP, tracing 101 pCIG2-transfected and 121 *Zac1*-transfected Tuj1$^+$ neurons. In E14.5–E18.5 pCIG2 control electroporations, almost all (98.9%) of the GFP$^+$Tuj1$^+$ neurons had two or more secondary branches extending out of the leading process (Fig. 5*C*,*C*′,*H*,*I*). In contrast, when *Zac1* was overexpressed, only 44.9% of GFP$^+$Tuj1$^+$ neurons elaborated branches in the CP (Fig. 5*D*,*D*′,*H*,*I*). Thus, *Zac1* overexpression prevents neurite branching, most notably in the CP, likely interfering with the final somal translocation of migrating neurons.

Concomitant with the dynamic changes in neurite branching patterns, intracellular organelles also undergo active movements in migrating neurons. The centrosome, which is located basal to the nucleus in a migrating neuron, first translocates into a swelling within the leading process, followed by the endoplasmic reticulum (ER). The centrosome then pulls the nuclear cage upward and the saltatory migratory movements are repeated (Fig. 5*J*). To examine whether organelle movements were disrupted during *Zac1* misexpression, we labeled the centrosome and ER by coelectroporating RFP–CENT2 (White et al., 2000) and pEF/Myc/ER/mCherry (Shim et al., 2008), respectively. In control pCIG2-transfected neurons, the centrosome (Fig. 5*K*,*K*′) and ER membranes (Fig. 5*M*,*M*′) were located on the basal side of the nucleus and were clearly in the process of translocating into the leading process. In contrast, in *Zac1*-overexpressing neurons, especially those with an amorphous shape, the centrosome (Fig. 5*L*,*L*′) and ER membranes (Fig. 5*N*,*N*′) remained on the apical side of the nucleus. These data suggest that organelle movements are perturbed in neurons that overexpress *Zac1*, likely contributing to the aberrant morphological transitions and migratory patterns of these neurons.

Neuronal migration is perturbed in *Zac1* mutant neocortices

ZAC1 is a critical developmental gene in humans, because both the increase and decrease in *ZAC1* expression in humans is associated with intellectual disability and smaller size for gestational age (e.g., Decipher identification numbers 248227 and 251465;

←

Figure 4. Altered migratory properties of *Zac1* overexpressing cortical cells. ***A–P***, Biphoton time-lapse microscopy of E15.5 cortical slice cultures electroporated with pCIG2 and pCIG2–*Zac1*. ***A***, ***B***, Photomicrographs of GFP$^+$ cells imaged 30 h after electroporation of pCIG2 (***A***) and pCIG2–*Zac1* (***B***). ***C–E***, Measurement of departure time defined as hours after transfection when GFP$^+$ cells left the GZ and entered the IZ (***C***). Departure times for 195 pCIG2 (white bars) and 133 pCIG2–*Zac1* (blue bars) transfected cells were recorded individually (***D***) and averaged (***E***). ***F–H***, Measurement of arrival time defined as hours after transfection when GFP$^+$ entered the CP (***F***). Arrival times for 195 pCIG2 (white bars) and 133 pCIG2–*Zac1* (blue bars) transfected cells were recorded individually (***G***) and averaged (***H***). ***I***, ***J***, Measurement of total distance (micrometers) migrated for 195 pCIG2 (white bars) and 133 pCIG2–*Zac1* (blue bars) transfected cells recorded individually (***I***) and averaged (***J***). ***K***, ***L***, Measurement of migration velocity (micrometers per hours) migrated for 195 pCIG2 (white bars) and 133 pCIG2–*Zac1* (blue bars) transfected cells recorded individually (***K***) and averaged (***L***). ***M***, ***N***, Quantitation of pauses in migration defined as any movement <3.5 μm over 2 consecutive hours of recording for 195 pCIG2 (white bars) and 133 pCIG2–*Zac1* (blue bars) individual transfected cells (***M***) and averaged (***N***). ***O***, ***P***, Quantitation of pause duration in hours for 195 pCIG2 (white bars) and 133 pCIG2–*Zac1* (blue bars) individual transfected cells (***O***) and averaged (***P***).

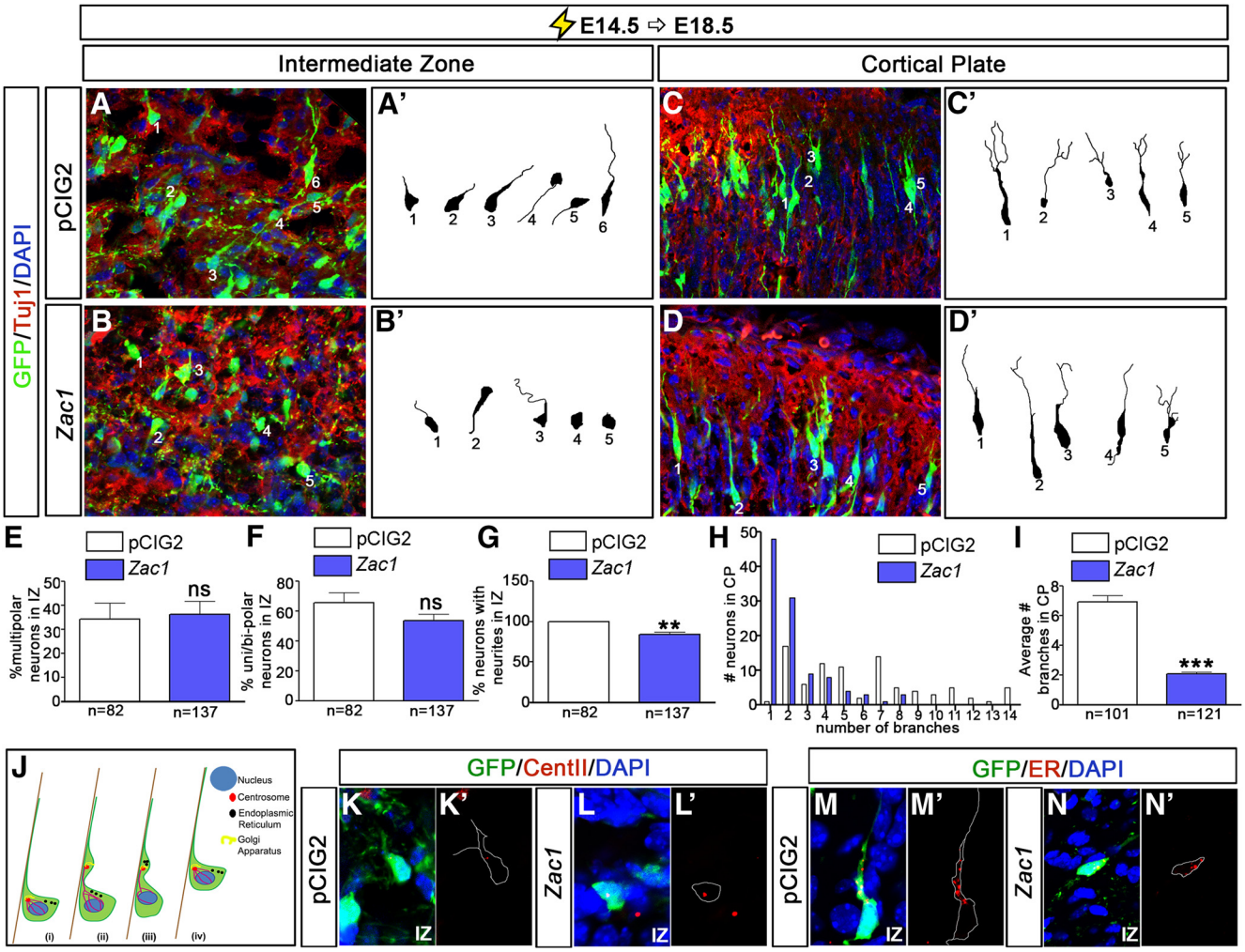

Figure 5. *Zac1* overexpression alters the morphology of migrating neurons. ***A–D***, E14.5–E18.5 electroporations of pCIG2 (***A***, ***C***; white bars) and pCIG2–*Zac1* (***B***, ***D***; blue bars). GFP $^{+}$Tuj1 $^{+}$ neurons (***A–D***) were traced (***A′–D′***) in the IZ (***A′***, ***B′***) and CP (***C′***, ***D′***) from pCIG2 ($n = 82$ in IZ; $n = 101$ in CP) and pCIG2–*Zac1* ($n = 137$ in IZ; $n = 121$ in CP) electroporations. ***E–I***, Quantitation of percentage multipolar neurons in the IZ (***E***), percentage unipolar/bipolar neurons in the IZ (***F***), percentage neurons with neurites in the IZ (***G***), number of branches per neuron in the CP (***H***), and average number of branches in the CP (***I***). ***J***, Schematic illustration of glial guided locomotion; saltatory movements begin with the centrosome, which is in front of the nucleus, and sends out microtubules to form a fork/cage around the nucleus (***i***). The leading process of the migrating neuron dilates and the centrosome enters (***ii***). Other organelles, such as the Golgi apparatus and ER, enter the dilated leading process (***iii***). Finally, microtubules attached to the centrosome pull the nucleus into the dilation (***iv***). ***K–N***, E14.5–E18.5 coelectroporations of pCIG2 (***K***, ***K′***, ***M***, ***M′***) or pCIG2–*Zac1* (***L***, ***L′***, ***N***, ***N′***) with RFP–CENT2 (***K***, ***K′***, ***L***, ***L′***) or pEF/Myc/ER/mCherry (***M***, ***M′***, ***N***, ***N′***). GFP $^{+}$ cells were traced in ***K′–N′*** to highlight the position of the organelles within the transfected cells. ns, Not significant.

Temple and Shield, 2002; Azzi et al., 2014). Growth restriction is also observed in *Zac1* mutant mice (Varrault et al., 2006). To determine whether the loss of *Zac1* expression also influenced neocortical development, we examined *Zac1* mutant mice. *Zac1* is a maternally imprinted gene (Piras et al., 2000; Smith et al., 2002). Consequently, crosses between *Zac1*$^{+/-}$ males and wild-type C57BL/6 females yield *Zac1*$^{+m/-}$ heterozygotes with a silenced, maternal wild-type allele; these embryos are effectively null for *Zac1* and are hereafter designated as *Zac1* mutants. We first examined *Zac1* mutant neocortices at E14.5 to determine whether proliferation and progenitor cell dynamics were altered. After a 30 min exposure to BrdU, similar numbers of progenitors were labeled in E14.5 *Zac1* mutant and wild-type cortices (Fig. 6*A–D*,*I*). In addition, there were no differences in the numbers of Pax6^{+} RGCs (Fig. 6*A*,*B*,*E*) and Tbr2^{+} INPs (Fig. 6*C*,*D*,*G*) in E14.5 *Zac1* mutants or in the numbers of progenitors that coexpressed Pax6/BrdU (Fig. 6*F*) or Tbr2/BrdU (Fig. 6*H*). To provide additional support for the lack of an effect of the *Zac1* mutation on progenitor cell maturation, we also analyzed progenitor populations at E15.5, 24 h after BrdU injection at E14.5. The ratios of Pax6/BrdU (Fig. 6*J*,*K*,*N*) and Tbr2/BrdU (Fig. 6*L*,*M*,*O*) coexpression, as well as the total BrdU counts (Fig. 6*P*), were not significantly different in E15.5 wild-type and *Zac1* mutants. Thus, the loss of *Zac1* does not alter the transition of cortical progenitors from Pax6^{+}BrdU^{+} RGCs to Tbr2^{+}Brdu^{+} INPs. So although *Zac1* is sufficient to block the RGC-to-INP transition and promote cell-cycle exit, it is not required for these events.

We next examined whether the loss of *Zac1* influenced neocortical neuronal migration. The majority of *Zac1* mutant pups die within 24 h after birth (Varrault et al., 2006; Ma et al., 2007b), precluding us from examining mature laminar patterns in *Zac1* mutants at postnatal day 7, when migration is normally complete. Nevertheless, we were able to analyze the initial partitioning of neurons into upper and deep layers of the cortex at E18.5 by BrdU birthdating. BrdU was administered at E14.5, when upper layer II–IV neurons are generated (Caviness, 1982; Caviness et al., 1995). The laminar positions of darkly labeled nuclei, corre-

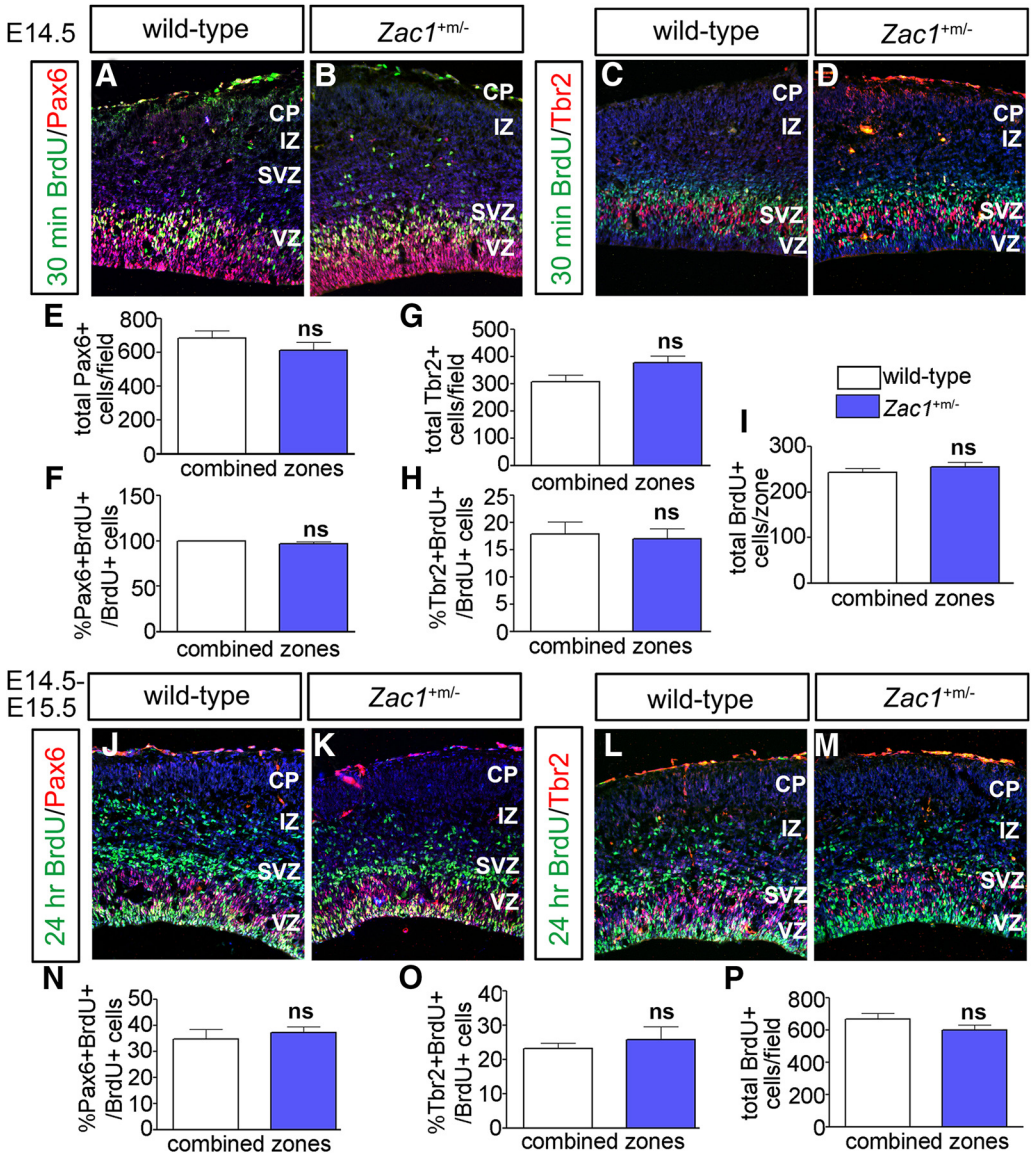

Figure 6. Loss of *Zac1* does not alter progenitor cell dynamics. ***A–I***, Analysis of Pax6/BrdU (***A***, ***B***) and Tbr2/BrdU (***C***, ***D***) coexpression in E14.5 wild-type and *Zac1* mutant (***B***) cortices after a 30 min BrdU pulse. DAPI labeling is blue counterstain. Quantitation of total number of Pax6 $^+$ cells (***E***), percentage Pax6 $^+$BrdU $^+$/BrdU $^+$ cells (***F***), total number of Tbr2 $^+$ cells (***G***), percentage Tbr2 $^+$BrdU $^+$/BrdU $^+$ cells (***H***), and total BrdU $^+$ cells (***I***) in wild-type ($n = 3$; white bars) and *Zac1* mutants ($n = 3$; blue bars). ***J–P***, Analysis of Pax6/BrdU (***J***, ***K***) and Tbr2/Brdu (***L***, ***M***) coexpression in E15.5 wild-type (***L***) and *Zac1* mutant (***M***) cortices after a 24 h BrdU pulse. DAPI labeling is blue counterstain. Quantitation of the percentage Pax6 $^+$BrdU $^+$/BrdU $^+$ cells (***N***), percentage Tbr2 $^+$BrdU $^+$/BrdU $^+$ cells (***O***), and total BrdU $^+$ cells (***P***) in wild types ($n = 3$; white bars) and *Zac1* mutants ($n = 3$; blue bars).

sponding to neurons derived from progenitors that underwent their last round of cell division immediately after labeling, were assessed at E18.5 (Fig. 7*A–C*). Cortical sections were subdivided into 13 10-μm bins, which were assigned to the VZ, IZ, or deep or upper CP layers based on differences in the size and distribution of DAPI $^+$ nuclei, and pairwise comparisons were made between wild-type and *Zac1* mutants. In wild-type cortices, the majority of labeled neurons were found in bins in upper layers II–IV (Fig. 7*A–A″*,*C*). In contrast, in *Zac1* mutants, fewer darkly stained nuclei were present in the upper-most cortical layers ($n = 3$; $p < 0.05$, *t* tests to compare bins; Fig. 7*B–B″*,*C*). Instead, a subset of the postmitotic cells labeled at E14.5 in *Zac1* mutants accumulated aberrantly in the upper GZ ($n = 3$; $p < 0.05$) and IZ ($n = 3$; $p < 0.001$; Fig. 7*B–B″*,*C*). Because progenitor cell maturation and neuronal differentiation were not notably different in *Zac1* mutants, these data suggested that some neurons born at E14.5 fail to migrate into the upper CP in the absence of *Zac1*, instead aggregating in deep positions in the GZ/IZ.

To confirm that the aberrantly aggregating cells in *Zac1* mutants were indeed neurons, we also examined the expression of layer-specific markers in E18.5 cortices. The total number of neurons expressing two upper layer markers—Beta3 (Fig. 7*D–F*), a basic-helix–loop–helix transcription factor expressed in layers II–V (Kim et al., 2002), and Cux1 (Fig. 7*H–J*), a Cut-like homeobox 1 transcription factor expressed in layers II–IV—were the same in E18.5 wild-type and *Zac1* mutant cortices. However, the distribution of Beta3 (Fig. 7*G*) and Cux1 $^+$ (Fig. 7*K*) neurons was altered in E18.5 *Zac1* mutants, with more of these neurons aberrantly aggregating in the GZ and IZ ($n = 3$; $p < 0.05$ for both Beta3 and Cux1 using *t* tests to compare bins; Fig. 7*G*,*K*). Cux1 was also found to be located ectopically in the deep regions of *Zac1* mutants ($n = 3$; $p < 0.05$; Fig. 6*K*). In contrast, Ctip2 (Bcl11b), a

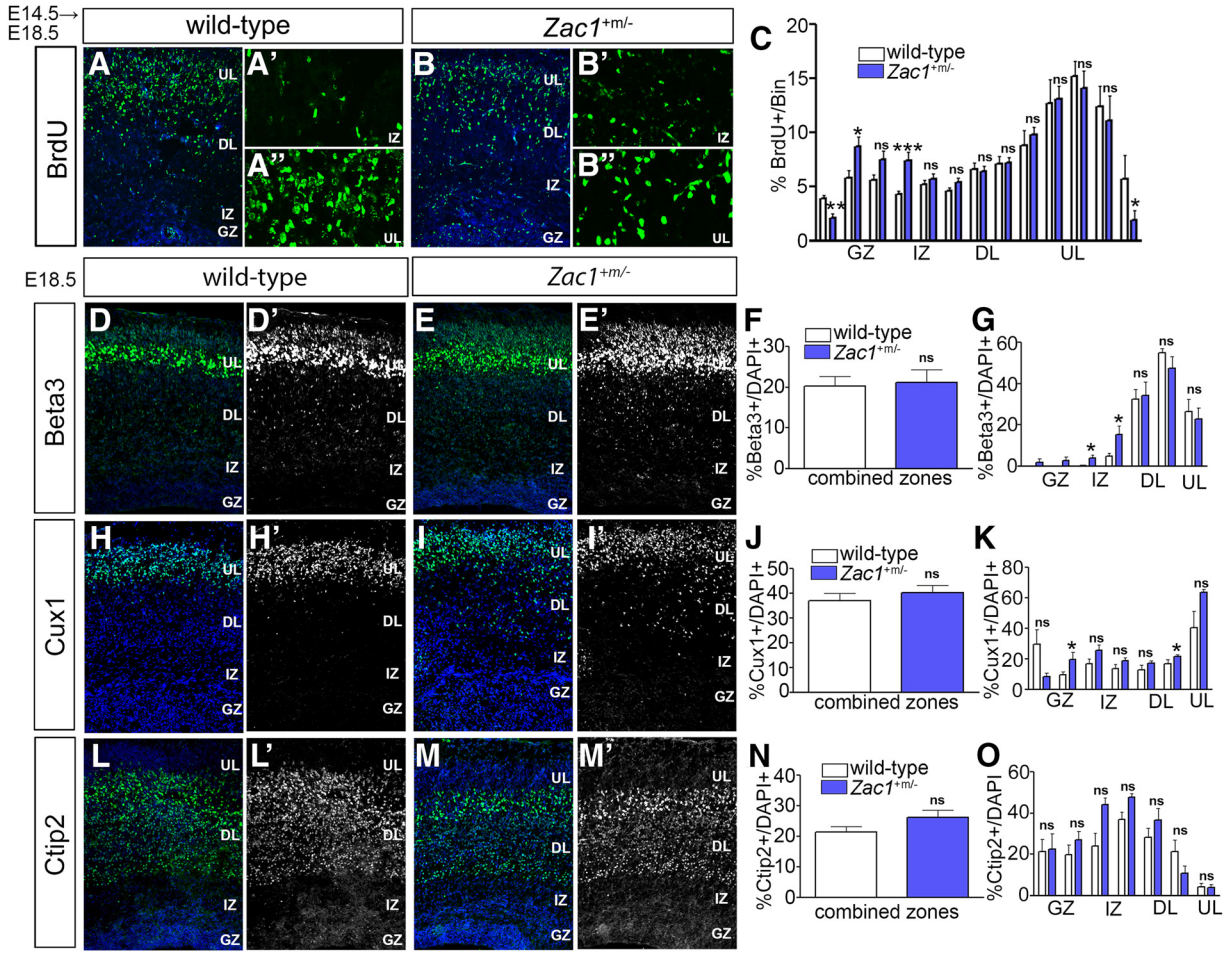

Figure 7. Aberrant distribution of laminar markers in *Zac1* mutant cortices. ***A–C***, E14.5–E18.5 BrdU birthdating in wild-type (***A–A″***) and *Zac1* mutant (***B–B″***) cortices. Distribution of BrdU-labeled cortical neurons divided into 13 bins corresponding to upper CP layers (bins 10–13), deep CP layers (bins 5–9), IZ (bins 3–4), and GZ (bins 1–2) in wild-type (white bars; $n = 3$) and *Zac1* mutant (blue bars; $n = 3$) cortices (***C***). ***D–N***, E18.5 wild-type (***D***, ***D′***, ***H***, ***H′***, ***L***, ***L′***) and *Zac1* mutant (***E***, ***E′***, ***I***, ***I′***, ***M***, ***M′***) cortices immunostained for Beta3 (***D***, ***D′***, ***E***, ***E′***), Cux1 (***H***, ***H′***, ***I***, ***I′***), and Ctip2 (***L***, ***L′***, ***M***, ***M′***). DAPI labeling is blue counterstain. Quantitation of percentage Beta3$^+$/DAPI$^+$ cells in total (***F***) and in each layer (***G***), percentage Cux1$^+$/DAPI$^+$ cells in total (***J***) and in each layer (***K***), and percentage Ctip2$^+$/DAPI$^+$ cells in total (***N***) and in each layer (***O***) for wild types ($n = 3$; white bars) and *Zac1* mutants ($n = 3$; blue bars).

layer V-specific transcription factor (Arlotta et al., 2005), was expressed in similar numbers of neurons and in a similar distribution throughout the cortical layers in both E18.5 wild-type and *Zac1* mutant cortices (Fig. 7*L–O*).

Thus, a small subset of late-born *Zac1* mutant neurons fail to migrate to their appropriate upper layers based on birthdating and laminar markers. Notably, these defects were overcome by P4, when cell counts revealed no differences in the number or distribution of upper layer neurons in the *Zac1* mutants that survived (data not shown). Hence, there is a delay, rather than a block, in upper layer neuronal migration in *Zac1* mutant neocortices.

Zac1 mutant neocortical neurons have aberrant morphologies

To further substantiate the requirement for *Zac1* in regulating the migration of upper layer neurons and to examine underlying causes, we performed two electroporation assays. First, we performed knockdown experiments. A highly efficient *Zac1*–shRNA construct [*Zac1*–sh(3); hereafter designated *Zac1*–shRNA] was identified by transfecting NIH-3T3 cells with four shRNA constructs carrying different *Zac1* target sequences (Fig. 8*A*). We then electroporated *Zac1*–shRNA or a scrambled shRNA control construct into E14.5 cortices and examined the distribution of electroporated cells at E18.5. Knockdown of *Zac1* had a striking effect on cell migration, with the vast majority of GFP$^+$ electroporated cells failing to migrate out of the GZ ($n = 3$; $p < 0.005$) and not reaching the IZ ($n = 3$; $p < 0.005$) and upper layers ($n = 3$; $p < 0.005$) of the neocortex (Fig. 8*B–D*). To confirm that *Zac1*–shRNA did not have off-target effects, we repeated the E14.5–E18.5 electroporations of sh-scrambled and sh-*Zac1* constructs in *Zac1* mutant cortices; neither shRNA construct blocked neuronal migration in *Zac1* mutants (Fig. 8*E*,*F*), indicating that *Zac1*–shRNA-induced migration errors are not off-target effects or an electroporation artifact. To assess whether a subset of neurons failed to migrate in *Zac1* mutant cortices, we used a second electroporation assay, introducing pCIG2 into E14.5 *Zac1* mutants and wild-type littermates and analyzing the distribution of GFP$^+$ cells at E18.5. In *Zac1* mutants, significantly more GFP$^+$ cells were found in deep cortical layers compared with wild-type controls ($n = 5$ for *Zac1* mutants and $n = 6$ for wild-type littermates; $p < 0.05$; Fig. 8*G–I*). Thus, there are subtle migratory defects in *Zac1* genetic mutants.

Next, to study the underlying cause of the migration defects in *Zac1* mutants in more detail, we examined the morphologies of pCIG2-transfected GFP$^+$Tuj1$^+$ neurons in the IZ and upper CP, comparing the with littermate controls. Within the IZ, there were no differences in the number of GFP$^+$Tuj1$^+$ multipolar neurons (Fig. 8*J*,*J′*,*K*,*K′*,*N*) or neurite-bearing neurons (Fig.

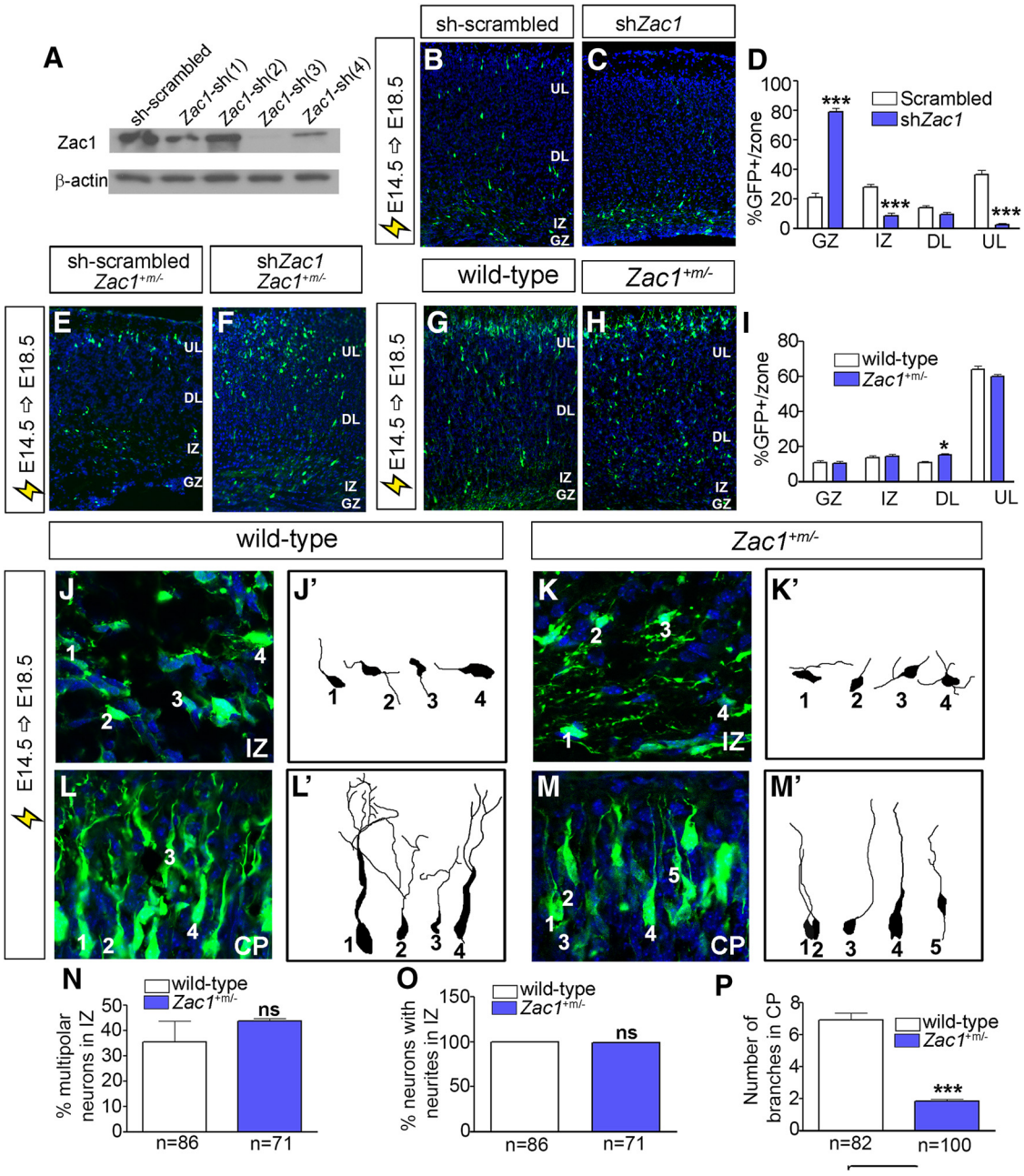

Figure 8. Aberrant morphology of migrating neurons in *Zac1* mutant cortices. ***A***, Western blot analysis of Zac1 and β-actin protein levels in NIH-3T3 cells cotransfected with pCIG2–*Zac1* along with different shRNA constructs. ***B–D***, E14.5–E18.5 electroporations of sh-scrambled control (***B***) and sh*Zac1* vectors (***C***) in wild-type CD1 timed pregnant females. Quantitation of percentage GFP $^{+}$ cells/layer for sh-scrambled ($n = 3$; white bars) and sh*Zac1* ($n = 3$; blue bars) (***D***). ***E***, ***F***, E14.5–E18.5 electroporations of *Zac1* mutant cortices with sh-scrambled and sh-*Zac1* constructs. ***G–I***, E14.5–E18.5 electroporation of pCIG2 in wild-type (***G***) and *Zac1* mutant (***H***) cortices. Quantitation of percentage GFP $^{+}$ cells in each layer for wild-type ($n = 3$; white bars) and *Zac1* mutant ($n = 3$; blue bars) cortices (***I***). ***J–P***, E14.5–E18.5 electroporation of pCIG2 in wild-type (***J***, ***L***) and *Zac1* mutant (***K***, ***M***) cortices, with images taken in the IZ (***J***, ***K***) and CP (***L***, ***M***). GFP $^{+}$Tuj1 $^{+}$ neurons in wild-type IZ (***J′***) and CP (***L′***) and in *Zac1*$^{+m/-}$ IZ (***K′***) and CP (***M′***) were traced. Quantitation of percentage multipolar neurons in IZ of wild-type ($n = 86$; white bars) and *Zac1* mutant ($n = 71$; blue bars) cortices (***N***). Quantitation of percentage neurons with neurites in the IZ of wild-type ($n = 86$; white bars) and *Zac1* mutant ($n = 71$; blue bars) cortices (***O***). Quantitation of the number of branches in the CP of wild-type ($n = 82$; white bars) and *Zac1* mutant ($n = 100$; blue bars) cortices (***P***). DL, Deep layer; UL, upper layer.

8*L*,*L*′,*M*,*M*′,*O*) in wild-type ($n = 86$) and *Zac1* mutant cortices ($n = 71$). However, many fewer branches were seen in the pCIG2-transfected GFP $^{+}$Tuj1 $^{+}$ neurons in *Zac1* mutant ($n = 100$; $p < 0.005$; Fig. 8*M*,*M*″,*P*) versus wild-type embryos ($n = 82$; Fig. 8*L*,*L*″,*P*) in the CP.

Combined, these data suggest that neuronal migration is perturbed when *Zac1* is knocked down and to a lesser extent when it is knocked out. However, there was a similar reduction in the branching of upper layer neurons in both genetic null mice and in transient knockdown experiments, suggesting that *Zac1* is absolutely required for this branching process, with no compensatory mechanisms in place. Given that similar branching defects were observed whether *Zac1* was overexpressed or underexpressed, we can conclude that *Zac1* is a dosage-sensitive gene, similar to other imprinted genes.

Zac1 regulates neuronal migration via *Pac1*

Because *Zac1* functions as a transcriptional activator or repressor (Varrault et al., 1998; Hoffmann et al., 2003), its effects on neuronal migration are likely mediated by downstream effectors.

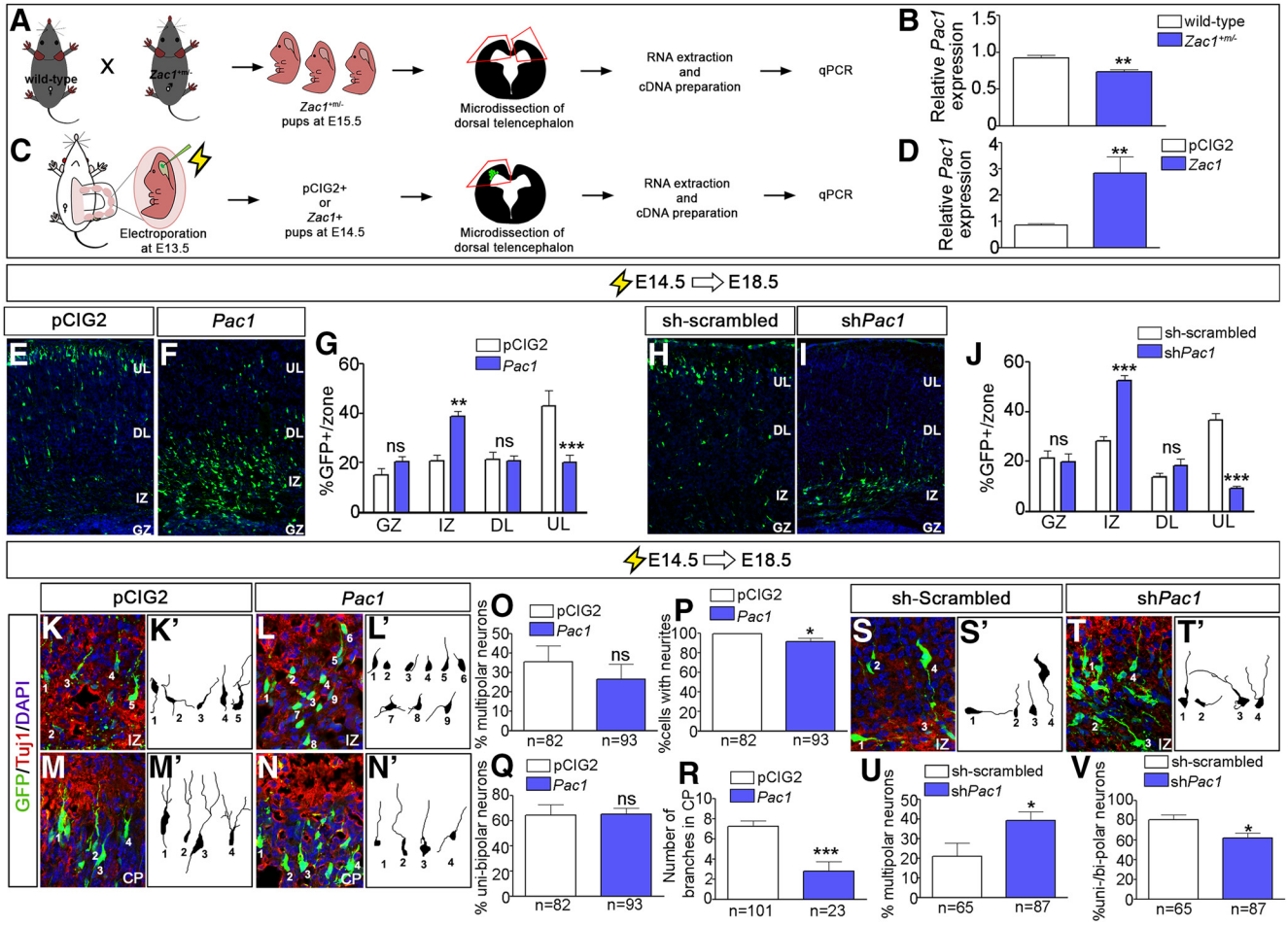

Figure 9. *Zac1* regulates neuronal migration by regulating *Pac1* transcription in the developing neocortex. ***A–D***, Schematic of the experimental design to test whether *Zac1* regulates the expression of Pac1 in E15.5 $Zac1^{+m/-}$ cortices (***A***) and in E13.5–E14.5 *Zac1* gain-of-function assays (***C***). Quantitation of qPCR data, showing reduced *Pac1* transcript levels in $Zac1^{+m/-}$ cortices [$n = 4$ for both wild-type (white bars) and *Zac1* mutant (blue bars); ***B***] and increased *Pac1* transcript levels after *Zac1* misexpression [$n = 6$ for both pCIG2 (white bars) and pCIG2–*Zac1* (blue bars); ***D***]. ***E–G***, E14.5–E18.5 electroporations of pCIG2 (***E***) and pCIG2-*Pac1* (***F***). Quantitation of percentage GFP $^+$ cells in each layer for pCIG2 control ($n = 3$; white bar) and pCIG2–Pac1 ($n = 3$; blue bar) (***G***). ***H–J***, E14.5–E18.5 electroporations of sh-scrambled (***H***) and sh*Pac1* (***I***). Quantitation of percentage GFP $^+$ cells in each layer for pCIG2 control ($n = 3$; white bar) and sh*Pac1* ($n = 3$; blue bar) (***J***). ***K–R***, E14.5–E18.5 electroporations of pCIG2 (***K***, ***M***) and pCIG2–*Pac1* (***L***, ***N***), showing coimmunolabeling of GFP (green) and Tuj1 (red). Blue is DAPI counterstain. Tracing of GFP $^+$Tuj1 $^+$ neurons in the IZ from pCIG2 control ($n = 82$; ***K′***) and pCIG2–*Pac1* ($n = 93$; ***L′***) electroporations. Quantitation of percentage multipolar cells (***O***), percentage cells with neurites (***P***), and percentage unipolar or bipolar neurons (***Q***) for pCIG2 control ($n = 3$; white bars) and pCIG2–*Pac1* ($n = 3$; blue bars). Tracing of GFP $^+$Tuj1 $^+$ neurons in the CP from pCIG2 control ($n = 101$; ***M′***) and pCIG2–*Pac1* ($n = 23$; ***N′***) electroporations. Quantitation of average number of branches per neuron in the CP (***R***). ***S–V***, E14.5–E18.5 electroporations of sh-scrambled (***S***) and sh*Pac1* (***T***), showing coimmunolabeling of GFP (green) and Tuj1 (red). Blue is DAPI counterstain. Tracing of GFP $^+$Tuj1 $^+$ neurons in the IZ from pCIG2 control ($n = 82$; ***S′***) and sh*Pac1* ($n = 87$; ***T′***). Quantitation of percentage multipolar neurons (***U***) and percentage unipolar or bipolar neurons (***V***) for sh-scrambled ($n = 3$; white bars) and sh*Zac1* ($n = 3$; blue bars).

Several *Zac1* transcriptional targets have been identified, including *Pac1* (Ciani et al., 1999; Rodríguez-Henche et al., 2002), which encodes a receptor for the neuropeptide PACAP. We focused on *Pac1* as a potential downstream effector of *Zac1* because *Pac1* is expressed at high levels in the neocortical VZ and to a lesser extent in the CP (Suh et al., 2001; Yan et al., 2013), similar to the *Zac1* expression profile (Fig. 1*A–F*). Moreover, PACAP promotes cell-cycle exit in cortical progenitors after E13.5 (Suh et al., 2001), mimicking the effects we observed during *Zac1* overexpression, although the authors did not examine whether *Pac1* also influenced neuronal migration.

To determine whether *Pac1* may be a downstream *Zac1* effector in the developing neocortex, we first asked whether *Zac1* regulated *Pac1* expression levels in this region of the neural tube. *Pac1* transcript levels were quantitated by qPCR in E18.5 microdissected wild-type ($n = 4$) and *Zac1* mutant ($n = 4$) neocortices, revealing a 1.2-fold decrease in *Zac1* mutants relative to wild type (Fig. 9*A*,*B*). Next, to test whether *Zac1* was sufficient to induce *Pac1* expression in neocortical cells, pCIG2 control ($n = 6$) and pCIG2-*Zac1* ($n = 6$) expression vectors were electroporated into E13.5 cortices and GFP $^+$ electroporated patches in the dorsal telencephalon were microdissected 24 h later (Fig. 9*C*,*D*). *Zac1* was upregulated 4.2-fold in *Zac1*-transfected cortical cells compared with control transfections, resulting in a 3.3-fold increase in *Pac1* transcript levels (Fig. 9*D*). Thus, *Zac1* is required and sufficient to regulate *Pac1* transcript levels in neocortical progenitors.

If *Zac1* acts via *Pac1* to regulate neuronal migration, we predicted that we would obtain the same perturbation of neuronal migration when *Pac1* was either overexpressed or knocked down. To test this hypothesis, we first electroporated pCIG2 control and pCIG2–*Pac1* expression vectors into E14.5 neocortices and harvested the embryos at E18.5 (Fig. 9*E*,*F*). In control electroporations, most GFP $^+$ cells had migrated to upper regions of the CP (Fig. 9*E*,*G*), whereas misexpression of *Pac1* led to the accumulation of more GFP $^+$ cells in the IZ ($n = 3$; $p < 0.01$) and fewer cells

reached upper layers of the CP ($n = 3$; $p < 0.005$; Fig. 9*F*,*G*). Therefore, *Pac1* misexpression phenocopies the migration defects observed when *Zac1* is misexpressed in E14.5 cortical progenitors (Fig. 1*J–L*). Next, to investigate whether *Pac1* loss-of-function phenocopied *Zac1* loss-of-function, we knocked down *Pac1* using shRNA, targeting E14.5 cortical progenitors and examining the positions of electroporated cells at E18.5. Relative to control electroporations (Fig. 9*H*,*J*), more GFP$^+$ cells electroporated with sh*Pac1* were ectopically located in the IZ ($n = 3$; $p < 0.005$) and fewer GFP$^+$ cells reached upper layers of the CP ($n = 3$; $p < 0.005$; Fig. 9*I*,*J*). Both the loss and gain of *Pac1* function thus perturbs neuronal migration, similar to the phenotypes observed when *Zac1* levels are manipulated.

As a final comparative measure of *Zac1* and *Pac1* functions, we examined the morphologies of cortical neurons after the overexpression or knockdown of *Pac1*. Similar to *Zac1*, overexpression of *Pac1* increased the number of GFP$^+$Tuj1$^+$ neurons that lacked neurites, with 9.6% of *Pac1*-transfected neurons acquiring an amorphous shape in the IZ ($n = 93$; $p < 0.005$; Fig. 9*K*,*K*′,*L*,*L*′,*P*). Also similar to *Zac1*, *Pac1* did not affect the multipolar-to-unipolar/bipolar ratio of the neurons that did extend neurites (Fig. 9*O*,*Q*). However, of the few GFP$^+$Tuj1$^+$ neurons that did reach the CP after *Pac1* overexpression, there was a reduction in the average number of neurite branches that were extended ($n = 23$; $p < 0.005$; Fig. 9*R*), similar to the *Zac1* gain-of-function phenotype. Conversely, when *Pac1* was knocked down by electroporating sh*Pac1* into E14.5 cortical progenitors (Fig. 9*S–V*), more GFP$^+$Tuj1$^+$ neurons acquired a multipolar shape compared with control transfections ($n = 87$ for sh*Pac1* vs $n = 63$ for sh-scrambled; $p < 0.05$; Fig. 9*U*), whereas fewer were bipolar ($p < 0.05$; Fig. 9*V*). Thus, *Pac1* is required for the multipolar-to-bipolar transition of locomoting neurons (Fig. 9*U*,*V*).

Together, these data indicate that *Pac1* transcription is regulated by *Zac1* in the neocortex and suggest that *Pac1* is necessary and sufficient downstream of *Zac1* to control the migratory behavior and morphologies of neocortical neurons.

Pac1 partially rescues migration defects associated with *Zac1* knockdown

To provide additional support for the idea that *Pac1* is a downstream effector of *Zac1* in the developing neocortex, we performed rescue experiments. For this purpose, we first conducted E14.5–E18.5 electroporations of pCIG2, pCIG2–*Zac1*, pCIG2–*Pac1*, sh-scrambled, sh*Zac1*, and sh*Pac1* constructs, confirming that the gain or loss of both *Zac1* and *Pac1* perturbed migration (Fig. 10*B–G*) and providing a comparative baseline for coelectroporation experiments. To provide a single measure of migration that could be compared between single and double electroporations, we calculated a migration index, dividing the cortex into seven bins of equal size, with the top-most bin, in which cells had migrated the farthest, given a value of 7, and the lowest bin, in which cells had migrated the least, assigned a value of 1 (Fig. 10*A*). The percentage of GFP$^+$ cells within each bin was then multiplied by the assigned bin value, and all numbers were added together. Using this strategy, the migration indices of pCIG2 ($n = 4$) and scrambled shRNA ($n = 3$) control transfections were 4.3 ± 0.2 and $5.0 \pm 0.1\%$, respectively (Fig. 10 *B*,*E*,*J*). In contrast, migration indices for pCIG2–*Zac1* (3.3 ± 1.5; $n = 3$; $p < 0.001$) and pCIG2–*Pac1* ($3.4 \pm 0.1\%$; $n = 3$; $p < 0.01$; Fig. 10*C*,*D*,*J*) were considerably lower than for pCIG2, whereas sh*Pac1* ($2.8 \pm 0.1\%$; $n = 4$; $p < 0.001$) and sh*Zac1* ($2.7 \pm 0.1\%$; $n = 3$; $p < 0.001$; Fig. 10*F*,*G*,*J*) were considerably lower than the scrambled shRNA control, as expected. Thus, we were able to use this migration index to compare the migratory effects of several constructs at once.

To determine whether *Pac1* was an essential *Zac1* effector, we first asked whether *Zac1* perturbed neuronal migration when *Pac1* was knocked down. The migration index for pCIG2–*Zac1* plus sh*Pac1* was $2.6 \pm 0.1\%$ ($n = 6$; Fig. 10*H*,*J*), even lower than that observed for the gain-of-function of *Zac1* ($p < 0.01$). Thus, *Zac1* gain-of-function perturbs radial migration even when *Pac1* is knocked down, suggesting that *Zac1* must control the expression of other migratory factors in addition to *Pac1*. We next asked the converse question: whether *Zac1* is required to initiate *Pac1* expression for normal migration to occur. Indeed, by knocking down *Zac1* and adding back *Pac1*, a rescue of neuronal migration defects was observed, with a resulting migration index of $4.2 \pm 0.1\%$ that was not significantly different from values observed in control electroporations ($n = 3$; $p > 0.05$; Fig. 10*I*,*J*). Given that the *Zac1* knockdown no longer perturbs migration when *Pac1* is overexpressed, we suggest that *Pac1* is indeed a critical downstream effector of *Zac1*. Together, these data support the notion that *Zac1* modulates neuronal migration at least in part by regulating the expression of *Pac1*, although other downstream effectors are also likely involved.

Discussion

Zac1 is a maternally imprinted, dosage-sensitive gene, and an increase or decrease in its expression is associated with developmental growth restriction and intellectual deficits in humans. Therefore, we investigated whether alterations in *Zac1* expression in the developing murine neocortex, which is the seat of higher-order cognitive functioning, would influence brain development. Striking defects in progenitor cell maturation, neuronal differentiation, neuronal morphology, and neuronal migration were observed during overexpression of *Zac1* in neocortical progenitors. Defects in neuronal migration were also observed in *Zac1* loss-of-function models, albeit to a lesser extent. Mechanistically, we attribute the ability of *Zac1* to control neocortical neuronal migration to its regulation of *Pac1*, a receptor for the neuropeptide PACAP that is known to regulate neocortical progenitor proliferation (Suh et al., 2001). Thus, we have uncovered a novel *Zac1–Pac1* regulatory circuit that plays an essential role in regulating progenitor proliferation, neuronal differentiation, and migration in the developing neocortex. Many of our conclusions are based on gain-of-function experiments, which can in some instances induce experimental artifacts. However, *Zac1* misexpression upregulates *Pac1* expression, a known *Zac1* transcriptional target, and *Zac1* and *Pac1* have similar gain-of-function phenotypes, thus supporting the specificity of our gain-of-function data. Moreover, because our goal was to mimic the increase in *Zac1* expression observed in human TNDM, it was necessary to use a gain-of-function approach.

Zac1 and the regulation of cortical progenitor cell proliferation

We found that *Zac1* misexpression reduces EdU incorporation in the neocortex and that fewer *Zac1*-overexpressing cells re-enter S-phase of the cell cycle. This is similar to our findings in the embryonic retina, in which *Zac1* misexpression also reduced S-phase progenitors (Ma et al., 2007b). *Zac1* similarly induces cell-cycle arrest in epithelial cell lines; conversely, *Zac1* expression is lost in several carcinomas that display an increased proliferative potential (Abdollahi, 2007). It is currently unknown how *Zac1* regulates cell-cycle exit, in either the developing CNS or tumorigenic cells, but it is thought to function independently of

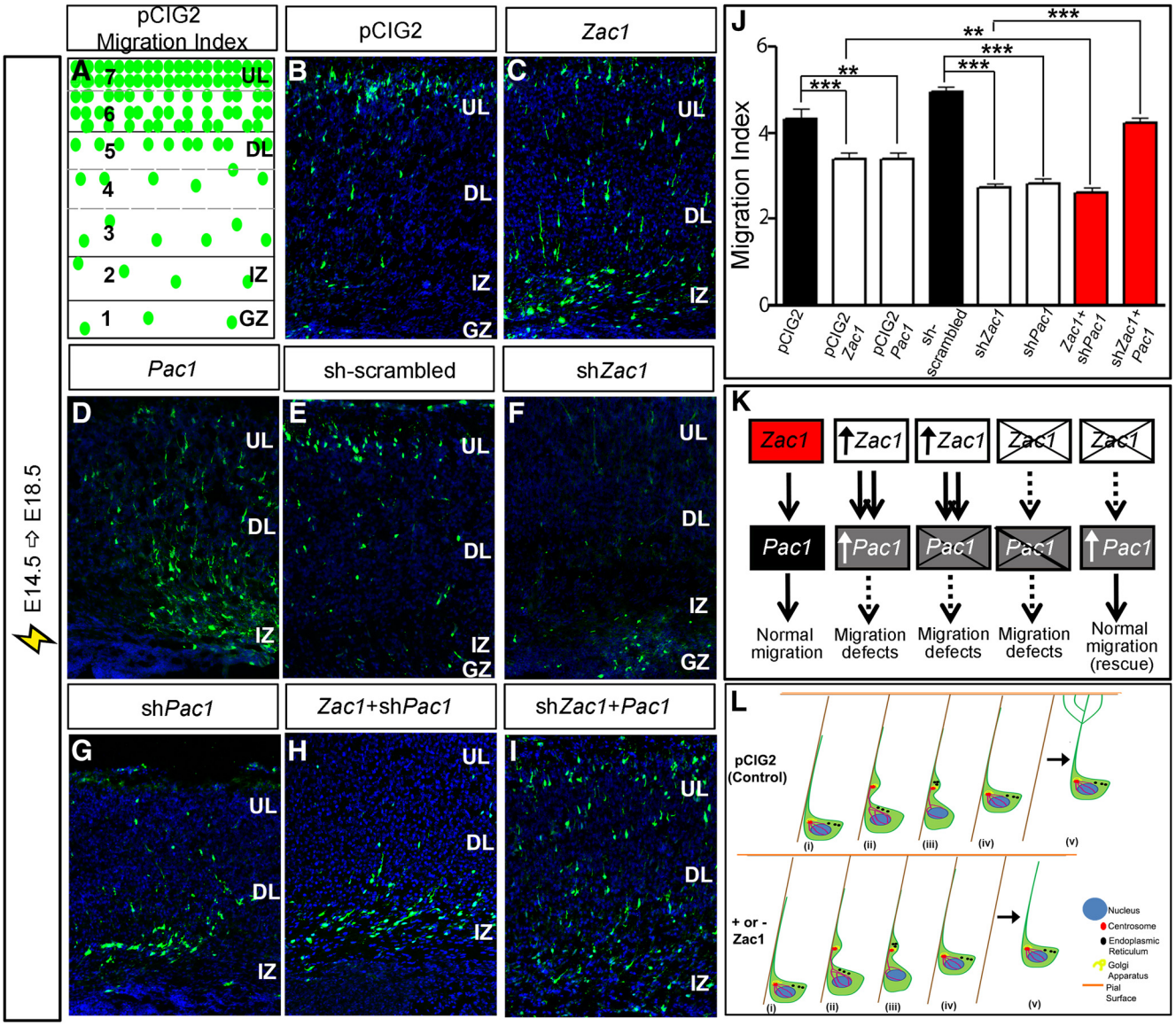

Figure 10. *Zac1* regulates neuronal migration via *Pac1* in the developing neocortex. ***A***, Schematic representation of method used to calculate migration index. ***B–F***, E14.5–E18.5 electroporations of pCIG2 (***B***), pCIG2–*Zac1* (***C***), pCIG2–*Pac1* (***D***), sh-scrambled (***E***), sh*Zac1* (***F***), sh*Pac1* (***G***), pCIG2–*Zac1* plus sh*Pac1* (***H***), and sh*Zac1* plus pCIG2–*Pac1* (***I***). ***J***, Quantitation of migration indices for all electroporations. ***K***, Summary of regulatory interactions between *Zac1* and *Pac1*. *Zac1* gain-of-function perturbs radial migration even when *Pac1* is knocked down, suggesting that *Zac1* controls the expression of other migratory factors. *Zac1* knockdown no longer perturbs migration when *Pac1* is overexpressed, suggesting that *Pac1* is the most critical regulator of migration downstream of *Zac1*. ***L***, Summary of the role of *Zac1* in guiding neuronal migration in the developing neocortex. At the end of glial guided locomotion (steps ***i–iv***), neurons detach from the radial glial scaffold and the leading process extends multiple branches that arborize to the pial surface (step ***v*** in pCIG2 control). In neurons in which *Zac1* expression is deregulated, branching of the leading process does not occur at the end of terminal translocation (step ***v***; + or − *Zac1*).

Kip-family cyclin dependent kinase inhibitors and retinoblastoma (Spengler et al., 1997). We found that *Zac1* promotes *Pac1* expression in cortical progenitors, whereas *Pac1* transcript levels were also reduced in *Zac1* mutant cortices, although to a lesser extent. PACAP has anti-proliferative properties in the developing neocortex, reducing the number of progenitors entering S-phase of the cell cycle at E13.5 and later (Suh et al., 2001). Therefore, the ability of *Zac1* to reduce proliferation is likely related to its ability to increase *Pac1* transcription. A similar model was proposed based on analyses of *Suz12* null cortices, which also display a reduction in cortical proliferation (Miró et al., 2009). *Suz12* encodes a component of a polycomb repressive complex 2 that regulates the expression of imprinted genes, such as *Zac1*. Accordingly, *Zac1* expression levels are upregulated in *Suz12* mutant cortices, as are the expression levels of *Pac1* (Miró et al., 2009). *Zac1* in turn has been shown to regulate the expression of a number of imprinted genes, including *Igf2*, *Dlk1*, and *H19*, all of which are associated with growth control and proliferation (Varrault et al., 2006). Future studies will be required to see whether these genes are also regulated by *Zac1* in the neocortex, accounting for the reduced proliferative capacity of *Zac1*-overexpressing cells. However, based on our studies, we can conclude that a *Zac1–Pac1* transcriptional pathway is a key regulator of progenitor cell proliferation in the developing neocortex.

Although we found that *Zac1* can promote cell-cycle exit, it was shown recently that *Zac1* can enhance the tumorigenicity of a glioma cell line, in contrast to its original identification as a tumor suppressor gene (Hide et al., 2009). This is perhaps not unexpected given that members of several gene families, including the *Runx* transcription factors (Cameron and Neil, 2004), Pten phos-

phatase (Groszer et al., 2001; Marino et al., 2002), and TGFβ signaling molecules (Bachman and Park, 2005), are lineage-specific oncogenes or tumor suppressors, depending on the time and tissue in which they are expressed. *Zac1* function is thus clearly context specific.

Zac1 blocks progenitor cell maturation and neuronal differentiation

We found that *Zac1* misexpression blocks the apical-to-basal transition of neocortical progenitors, leading to the sustained expression of Pax6 and a reduction in Tbr2 expression. Furthermore, neuronal differentiation was delayed, but not completely blocked, by the overexpression of *Zac1* in neocortical progenitors. The ability of *Zac1* to block neocortical cells as early apical progenitors is consistent with a recent study in a glioma cell line, in which *Zac1* promoted the expression of nestin, a marker of apical radial glia, and blocked neuronal differentiation (Hide et al., 2009). However, it is not clear whether *Zac1* is a direct transcriptional regulator of apical progenitor genes, such as *Nestin* or *Pax6*, or whether it alters the expression of other genes that block progenitor cell maturation and neuronal differentiation (e.g., *Pac1*). Interestingly, *Zac1* and *Pax6* expression have very similar expression domains in the embryonic telencephalon, consistent with a potential regulatory interaction (Alam et al., 2005). Interestingly, *Pax6* expression was reduced in the embryonic pancreas of a transgenic mouse engineered to overexpress a locus associated with TNDM, which included *ZAC1* (Ma et al., 2004), suggesting a repressive interaction between *Zac1* and *Pax6*. Indeed, Zac1 is known to function both as a transcriptional activator and repressor (Huang and Stallcup, 2000; Hoffmann et al., 2003). Additional studies are required to explore potential regulatory interactions between *Zac1* and *Pax6*.

Zac1 regulates neocortical neuronal migration via *Pac1*

We found that *Zac1* misexpression at E12.5 did not perturb neuronal migration, whereas misexpression of *Zac1* at E14.5 prevented neurons from migrating out of the GZ and IZ and into the CP. Other studies have identified two temporal phases of neuronal migration: (1) an early period of somal translocation that occurs before E14.5; and (2) a later period of glial-guided locomotion that primarily occurs after E14.5 (Nadarajah et al., 2001). Based on the timing of its effects, *Zac1* overexpression influences the latter period of locomotion. Indeed, several of the changes that locomoting neurons undergo were perturbed when *Zac1* was overexpressed, including an increase in the length and number of pauses, and reduced neuronal branching in the IZ, in which a multipolar shape is associated with the waiting period. *Zac1*-overexpressing neurons also displayed decreased branching patterns in the upper CP, in which the final movement of neurons into their laminar position depends on somal translocation, with the force required for movement generated by the branching of the primary dendrites and their attachment to the pial surface.

Analyses of *Zac1* mutant cortices also revealed defects in neocortical neuronal migration, albeit less severe than in our gain-of-function models. Consistent with this observation, we previously identified a role for *Zac1* in mediating neuronal migration in the developing retina (Ma et al., 2007b). In addition, in the *Zac1* mutant cerebellum, fewer neurons are found in medial cerebellar nuclei, and fewer Golgi cells populate cerebellar lobule IX, possibly also reflecting a neuronal migration defect (Chung et al., 2011). Consistent with the idea that *Zac1* may mediate its effects on neuronal migration through *Pac1* signaling, PACAP reduces the rate of granule cell migration in culture (Falluel-Morel et al., 2005; Cameron et al., 2009). Together, our data suggest that neuronal migration may be regulated by different signaling pathways early and late in corticogenesis.

Several *Zac1* transcriptional targets have been identified, including *Tcf4* (Schmidt-Edelkraut et al., 2014), *Pparg1* (Barz et al., 2006), *Cdkn1a* (Liu, 2011), *Rasgfr1* (Hoffmann and Spengler, 2012), *Glut4* (Czubryt et al., 2010), and *Pac1* (Ciani et al., 1999; Rodríguez-Henche et al., 2002). We focused on *Pac1* as a potential downstream effector of *Zac1* for several reasons. First, the overexpression of *Pac1* signaling molecules in humans has been associated with developmental brain disorders (Cameron et al., 2009). Second, previous time-lapse video microscopy studies have shown that PACAP1–38, a *Pac1* agonist, delays the migration of cerebellar granule cells (Falluel-Morel et al., 2005; Cameron et al., 2009). In contrast, PACAP6–38, a *Pac1* antagonist, has no effect (Falluel-Morel et al., 2005; Cameron et al., 2009), and the overall laminar organization of the cerebellum is normal in *PACAP* mutant mice, indicating that this neuropeptide is sufficient but not required to regulate the migration of cerebellar granule cells (Allais et al., 2007). In contrast, in this study, we observe neuronal migration defects after *Pac1* gain- and loss-of-function in the neocortex, suggesting that precise levels of signaling through this receptor is required for normal migration of neocortical neurons. Notably, *Pac1* perturbations phenocopied those observed when *Zac1* expression was altered, and misexpression of *Pac1* could rescue the *Zac1* knockdown migratory phenotype, suggesting that these genes act in the same genetic pathway. Conversely, when *Zac1* was overexpressed and *Pac1* was knocked down, migratory defects were not rescued, suggesting that *Zac1* induces the expression of other downstream genes that perturb migration. Future experiments will be required to identify the exact nature of these genes and the underlying regulatory interactions.

Together, these data increase our understanding of the pathways that regulate the morphogenetic changes associated with neuronal differentiation and migration in the neocortex.

References

Abdollahi A (2007) LOT1 (ZAC1/PLAGL1) and its family members: mechanisms and functions. J Cell Physiol 210:16–25. CrossRef Medline

Alam S, Zinyk D, Ma L, Schuurmans C (2005) Members of the Plag gene family are expressed in complementary and overlapping regions in the developing murine nervous system. Dev Dyn 234:772–782. CrossRef Medline

Allais A, Burel D, Isaac ER, Gray SL, Basille M, Ravni A, Sherwood NM, Vaudry H, Gonzalez BJ (2007) Altered cerebellar development in mice lacking pituitary adenylate cyclase-activating polypeptide. Eur J Neurosci 25:2604–2618. CrossRef Medline

Anderson AA, Helmering J, Juan T, Li CM, McCormick J, Graham M, Baker DM, Damore MA, Véniant MM, Lloyd DJ (2009) Pancreatic islet expression profiling in diabetes-prone C57BLKS/J mice reveals transcriptional differences contributed by DBA loci, including Plagl1 and Nnt. Pathogenetics 2:1. CrossRef Medline

Arima T, Wake N (2006) Establishment of the primary imprint of the HYMAI/PLAGL1 imprint control region during oogenesis. Cytogenet Genome Res 113:247–252. CrossRef Medline

Arlotta P, Molyneaux BJ, Chen J, Inoue J, Kominami R, Macklis JD (2005) Neuronal subtype-specific genes that control corticospinal motor neuron development in vivo. Neuron 45:207–221. CrossRef Medline

Azzi S, Sas TC, Koudou Y, Le Bouc Y, Souberbielle JC, Dargent-Molina P, Netchine I, Charles MA (2014) Degree of methylation of ZAC1 (PLAGL1) is associated with prenatal and post-natal growth in healthy infants of the EDEN mother child cohort. Epigenetics 9:338–345. CrossRef Medline

Bachman KE, Park BH (2005) Duel nature of TGF-beta signaling: tumor suppressor vs. tumor promoter. Curr Opin Oncol 17:49–54. CrossRef Medline

Barz T, Hoffmann A, Panhuysen M, Spengler D (2006) Peroxisome

proliferator-activated receptor gamma is a Zac target gene mediating Zac antiproliferation. Cancer Res 66:11975–11982. CrossRef Medline

Basyuk E, Coulon V, Le Digarcher A, Coisy-Quivy M, Moles JP, Gandarillas A, Journot L (2005) The candidate tumor suppressor gene ZAC is involved in keratinocyte differentiation and its expression is lost in basal cell carcinomas. Mol Cancer Res 3:483–492. CrossRef Medline

Britz O, Mattar P, Nguyen L, Langevin LM, Zimmer C, Alam S, Guillemot F, Schuurmans C (2006) A role for proneural genes in the maturation of cortical progenitor cells. Cereb Cortex 16:i138–i151. CrossRef Medline

Cameron DB, Raoult E, Galas L, Jiang Y, Lee K, Hu T, Vaudry D, Komuro H (2009) Role of PACAP in controlling granule cell migration. Cerebellum 8:433–440. CrossRef Medline

Cameron ER, Neil JC (2004) The Runx genes: lineage-specific oncogenes and tumor suppressors. Oncogene 23:4308–4314. CrossRef Medline

Caviness VS Jr (1982) Neocortical histogenesis in normal and reeler mice: a developmental study based upon [^{3}H]thymidine autoradiography. Brain Res 256:293–302. Medline

Caviness VS Jr, Takahashi T, Nowakowski RS (1995) Numbers, time and neocortical neuronogenesis: a general developmental and evolutionary model. Trends Neurosci 18:379–383. CrossRef Medline

Chung SH, Marzban H, Aldinger K, Dixit R, Millen K, Schuurmans C, Hawkes R (2011) Zac1 plays a key role in the development of specific neuronal subsets in the mouse cerebellum. Neural Dev 6:25. CrossRef Medline

Ciani E, Hoffmann A, Schmidt P, Journot L, Spengler D (1999) Induction of the PAC1-R (PACAP-type I receptor) gene by p53 and Zac. Brain Res Mol Brain Res 69:290–294. CrossRef Medline

Czubryt MP, Lamoureux L, Ramjiawan A, Abrenica B, Jangamreddy J, Swan K (2010) Regulation of cardiomyocyte Glut4 expression by ZAC1. J Biol Chem 285:16942–16950. CrossRef Medline

Diplas AI, Lambertini L, Lee MJ, Sperling R, Lee YL, Wetmur J, Chen J (2009) Differential expression of imprinted genes in normal and IUGR human placentas. Epigenetics 4:235–240. CrossRef Medline

Dixit R, Lu F, Cantrup R, Gruenig N, Langevin LM, Kurrasch DM, Schuurmans C (2011) Efficient gene delivery into multiple CNS territories using in utero electroporation. J Vis Exp pii:2957. CrossRef Medline

Englund C, Fink A, Lau C, Pham D, Daza RA, Bulfone A, Kowalczyk T, Hevner RF (2005) Pax6, Tbr2, and Tbr1 are expressed sequentially by radial glia, intermediate progenitor cells, and postmitotic neurons in developing neocortex. J Neurosci 25:247–251. CrossRef Medline

Falluel-Morel A, Vaudry D, Aubert N, Galas L, Bernard M, Basille M, Fontaine M, Fournier A, Vaudry H, Gonzales BJ (2005) Effects of PACAP and C2-ceramide on motility of cerebellar granule neurons: the fastest is not the farthest (in French). Med Sci 21:696–698. CrossRef Medline

Fattal-Valevski A, Toledano-Alhadef H, Leitner Y, Geva R, Eshel R, Harel S (2009) Growth patterns in children with intrauterine growth retardation and their correlation to neurocognitive development. J Child Neurol 24:846–851. CrossRef Medline

Geva R, Eshel R, Leitner Y, Fattal-Valevski A, Harel S (2006a) Memory functions of children born with asymmetric intrauterine growth restriction. Brain Res 1117:186–194. CrossRef Medline

Geva R, Eshel R, Leitner Y, Valevski AF, Harel S (2006b) Neuropsychological outcome of children with intrauterine growth restriction: a 9-year prospective study. Pediatrics 118:91–100. CrossRef Medline

Groszer M, Erickson R, Scripture-Adams DD, Lesche R, Trumpp A, Zack JA, Kornblum HI, Liu X, Wu H (2001) Negative regulation of neural stem/progenitor cell proliferation by the Pten tumor suppressor gene in vivo. Science 294:2186–2189. CrossRef Medline

Hand R, Bortone D, Mattar P, Nguyen L, Heng JI, Guerrier S, Boutt E, Peters E, Barnes AP, Parras C, Schuurmans C, Guillemot F, Polleux F (2005) Phosphorylation of Neurogenin2 specifies the migration properties and the dendritic morphology of pyramidal neurons in the neocortex. Neuron 48:45–62. CrossRef Medline

Hide T, Takezaki T, Nakatani Y, Nakamura H, Kuratsu J, Kondo T (2009) Sox11 prevents tumorigenesis of glioma-initiating cells by inducing neuronal differentiation. Cancer Res 69:7953–7959. CrossRef Medline

Hoffmann A, Spengler D (2012) Transient neonatal diabetes mellitus gene Zac1 impairs insulin secretion in mice through Rasgrf1. Mol Cell Biol 32:2549–2560. CrossRef Medline

Hoffmann A, Ciani E, Boeckardt J, Holsboer F, Journot L, Spengler D (2003) Transcriptional activities of the zinc finger protein Zac are differentially controlled by DNA binding. Mol Cell Biol 23:988–1003. CrossRef Medline

Huang SM, Stallcup MR (2000) Mouse Zac1, a transcriptional coactivator and repressor for nuclear receptors. Mol Cell Biol 20:1855–1867. CrossRef Medline

Kamikihara T, Arima T, Kato K, Matsuda T, Kato H, Douchi T, Nagata Y, Nakao M, Wake N (2005) Epigenetic silencing of the imprinted gene ZAC by DNA methylation is an early event in the progression of human ovarian cancer. Int J Cancer 115:690–700. CrossRef Medline

Kim MH, Gunnersen J, Augustine C, Tan SS (2002) Region-specific expression of the helix-loop-helix gene BETA3 in developing and adult brains. Mech Dev 114:125–128. CrossRef Medline

Langevin LM, Mattar P, Scardigli R, Roussigné M, Logan C, Blader P, Schuurmans C (2007) Validating in utero electroporation for the rapid analysis of gene regulatory elements in the murine telencephalon. Dev Dyn 236:1273–1286. CrossRef Medline

Li S, Mattar P, Zinyk D, Singh K, Chaturvedi CP, Kovach C, Dixit R, Kurrasch DM, Ma YC, Chan JA, Wallace V, Dilworth FJ, Brand M, Schuurmans C (2012) GSK3 temporally regulates neurogenin 2 proneural activity in the neocortex. J Neurosci 32:7791–7805. CrossRef Medline

Liu JS (2011) Molecular genetics of neuronal migration disorders. Curr Neurol Neurosci Rep 11:171–178. CrossRef Medline

Ma D, Shield JP, Dean W, Leclerc I, Knauf C, Burcelin R Ré, Rutter GA, Kelsey G (2004) Impaired glucose homeostasis in transgenic mice expressing the human transient neonatal diabetes mellitus locus, TNDM. J Clin Invest 114:339–348. CrossRef Medline

Ma L, Hocking JC, Hehr CL, Schuurmans C, McFarlane S (2007a) Zac1 promotes a Muller glial cell fate and interferes with retinal ganglion cell differentiation in *Xenopus* retina. Dev Dyn 236:192–202. CrossRef Medline

Ma L, Cantrup R, Varrault A, Colak D, Klenin N, Götz M, McFarlane S, Journot L, Schuurmans C (2007b) Zac1 functions through TGFbetaII to negatively regulate cell number in the developing retina. Neural Dev 2:11. CrossRef Medline

Marino S, Krimpenfort P, Leung C, van der Korput HA, Trapman J, Camenisch I, Berns A, Brandner S (2002) PTEN is essential for cell migration but not for fate determination and tumourigenesis in the cerebellum. Development 129:3513–3522. Medline

Mattar P, Britz O, Johannes C, Nieto M, Ma L, Rebeyka A, Klenin N, Polleux F, Guillemot F, Schuurmans C (2004) A screen for downstream effectors of Neurogenin2 in the embryonic neocortex. Dev Biol 273:373–389. CrossRef Medline

Miró X, Zhou X, Boretius S, Michaelis T, Kubisch C, Alvarez-Bolado G, Gruss P (2009) Haploinsufficiency of the murine polycomb gene Suz12 results in diverse malformations of the brain and neural tube. Dis Model Mech 2:412–418. CrossRef Medline

Nadarajah B, Brunstrom JE, Grutzendler J, Wong RO, Pearlman AL (2001) Two modes of radial migration in early development of the cerebral cortex. Nat Neurosci 4:143–150. CrossRef Medline

Nadarajah B, Alifragis P, Wong RO, Parnavelas JG (2003) Neuronal migration in the developing cerebral cortex: observations based on real-time imaging. Cereb Cortex 13:607–611. CrossRef Medline

Noctor SC, Martínez-Cerdeño V, Ivic L, Kriegstein AR (2004) Cortical neurons arise in symmetric and asymmetric division zones and migrate through specific phases. Nat Neurosci 7:136–144. CrossRef Medline

Peleg D, Kennedy CM, Hunter SK (1998) Intrauterine growth restriction: identification and management. Am Fam Physician 58:453–460, 466–457. Medline

Piras G, El Kharroubi A, Kozlov S, Escalante-Alcalde D, Hernandez L, Copeland NG, Gilbert DJ, Jenkins NA, Stewart CL (2000) Zac1 (Lot1), a potential tumor suppressor gene, and the gene for epsilon-sarcoglycan are maternally imprinted genes: identification by a subtractive screen of novel uniparental fibroblast lines. Mol Cell Biol 20:3308–3315. CrossRef Medline

Rodríguez-Henche N, Jamen F, Leroy C, Bockaert J, Brabet P (2002) Transcription of the mouse PAC1 receptor gene: cell-specific expression and regulation by Zac1. Biochim Biophys Acta 1576:157–162. CrossRef Medline

Schmidt-Edelkraut U, Daniel G, Hoffmann A, Spengler D (2014) Zac1 regulates cell cycle arrest in neuronal progenitors via Tcf4. Mol Cell Biol 34:1020–1030. CrossRef Medline

Sessa A, Mao CA, Hadjantonakis AK, Klein WH, Broccoli V (2008) Tbr2 directs conversion of radial glia into basal precursors and guides neuronal amplification by indirect neurogenesis in the developing neocortex. Neuron 60:56–69. CrossRef Medline

Shim SY, Wang J, Asada N, Neumayer G, Tran HC, Ishiguro K, Sanada K,

Nakatani Y, Nguyen MD (2008) Protein 600 is a microtubule/endoplasmic reticulum-associated protein in CNS neurons. J Neurosci 28: 3604–3614. CrossRef Medline

Smith RJ, Arnaud P, Konfortova G, Dean WL, Beechey CV, Kelsey G (2002) The mouse Zac1 locus: basis for imprinting and comparison with human ZAC. Gene 292:101–112. CrossRef Medline

Spengler D, Villalba M, Hoffmann A, Pantaloni C, Houssami S, Bockaert J, Journot L (1997) Regulation of apoptosis and cell cycle arrest by Zac1, a novel zinc finger protein expressed in the pituitary gland and the brain. EMBO J 16:2814–2825. CrossRef Medline

Suh J, Lu N, Nicot A, Tatsuno I, DiCicco-Bloom E (2001) PACAP is an anti-mitogenic signal in developing cerebral cortex. Nat Neurosci 4: 123–124. CrossRef Medline

Tabata H, Nakajima K (2003) Multipolar migration: the third mode of radial neuronal migration in the developing cerebral cortex. J Neurosci 23:9996–10001. Medline

Tanaka T, Serneo FF, Higgins C, Gambello MJ, Wynshaw-Boris A, Gleeson JG (2004) Lis1 and doublecortin function with dynein to mediate coupling of the nucleus to the centrosome in neuronal migration. J Cell Biol 165:709–721. CrossRef Medline

Temple IK, Shield JP (2002) Transient neonatal diabetes, a disorder of imprinting. J Med Genet 39:872–875. CrossRef Medline

Touahri Y, Adnani L, Mattar P, Markham K, Klenin N, Schuurmans C (2015) Non-isotopic RNA in situ hybridization on embryonic sections. Curr Protoc Neurosci 70:1.22.1–1.22.25. CrossRef Medline

Varrault A, Ciani E, Apiou F, Bilanges B, Hoffmann A, Pantaloni C, Bockaert J, Spengler D, Journot L (1998) hZAC encodes a zinc finger protein with antiproliferative properties and maps to a chromosomal region frequently lost in cancer. Proc Natl Acad Sci U S A 95:8835–8840. CrossRef Medline

Varrault A, Gueydan C, Delalbre A, Bellmann A, Houssami S, Aknin C, Severac D, Chotard L, Kahli M, Le Digarcher A, Pavlidis P, Journot L (2006) Zac1 regulates an imprinted gene network critically involved in the control of embryonic growth. Dev Cell 11:711–722. CrossRef Medline

White RA, Pan Z, Salisbury JL (2000) GFP-centrin as a marker for centriole dynamics in living cells. Microsc Res Tech 49:451–457. CrossRef Medline

Wilkinson LS, Davies W, Isles AR (2007) Genomic imprinting effects on brain development and function. Nat Rev Neurosci 8:832–843. CrossRef Medline

Yan Y, Zhou X, Pan Z, Ma J, Waschek JA, DiCicco-Bloom E (2013) Pro- and anti-mitogenic actions of pituitary adenylate cyclase-activating polypeptide in developing cerebral cortex: potential mediation by developmental switch of PAC1 receptor mRNA isoforms. J Neurosci 33:3865–3878. CrossRef Medline

Yuasa S, Onizuka T, Shimoji K, Ohno Y, Kageyama T, Yoon SH, Egashira T, Seki T, Hashimoto H, Nishiyama T, Kaneda R, Murata M, Hattori F, Makino S, Sano M, Ogawa S, Prall OW, Harvey RP, Fukuda K (2010) Zac1 is an essential transcription factor for cardiac morphogenesis. Circ Res 106:1083–1091. CrossRef Medline